Title

I. SOME MEASUREMENTS OF MAGNETIC HYPERFINE HEAT CAPACITIES. II. HEAT CAPACITIES OF COPPER-MANGANESE ALLOYS BELOW 1|K

Author

Ho, James Chien-Ming.

Publication Date

1965-09-01

University of California

Ernest O. Lawrence Radiation Laboratory

I. SOME MEASUREMENTS OF MAGNETIC HYPERFINE HEAT CAPACITIES
II. HEAT CAPACITIES OF COPPER-MANGANESE ALLOYS BELOW 1°K

Berkeley, California

DISCLAIMER

Research and Development

UCRL-16180

UNIVERSITY OF CALIFORNIA

Lawrence Radiation Laboratory
Berkeley, California

AEC Contract W-7405-eng-48

I. SOME MEASUREMENTS OF MAGNETIC HYPERFINE HEAT CAPACITIES

II. HEAT CAPACITIES OF COPPER-MANGANESE ALLOYS BELOW 1°K

James Chien-Ming Ho

(Ph.D. Thesis)

September 1965

TABLE OF CONTENTS

Table of Contents (Continued)

I. SOME MEASUREMENTS OF MAGNETIC HYPERFINE HEAT CAPACITIES

II. HEAT CAPACITIES OF COPPER-MANGANESE ALLOYS BELOW 1°K

James Chien-Ming Ho

Inorganic Materials Research Division
Lawrence Radiation Laboratory
and Department of Chemistry
University of California, Berkeley, California

ABSTRACT

September 1965

I

The hyperfine fields at Mn nuclei in antiferromagnetic γ-manganese and gold-manganese have been calorimetrically determined to be 65 kOe and 320 kOe, respectively. For antiferromagnetic chromium, however, the magnetic hyperfine heat capacity was not observed at temperatures as low as 0.06°K, and only an upper limit to the hyperfine field at Cr nuclei, 13 kOe, could be obtained. All these values are smaller than that expected from the results for the ferromagnets of the iron series, iron, cobalt, and nickel. This apparent difference might be due to the 4s-electron contribution or to the exchange polarization of the 3s-electrons of one ion by the 3d-electrons of its neighbours.

The magnetic hyperfine heat capacities of two alloys containing respectively 0.75 at.% Os and 3.21 at.% Pt dissolved in Fe have also been measured. The hyperfine fields at the nuclei were found to be 1400 kOe for Os and 1390 kOe for Pt.

II

Measurements of the heat capacities of dilute manganese in copper alloys have been made below 1°K to determine the contribution to the

low-temperature heat capacity that is associated with the magnetic ordering process. The theoretical low-temperature limit for this anomaly, which is linear in temperature and independent of manganese concentration, was not observed, although the heat capacity was found to be remarkably insensitive to manganese concentration.

The heat capacities of several higher manganese content copper-manganese alloys have also been determined. For all samples used in this work, which cover the whole composition range of the copper-manganese system, the hyperfine fields H_e at Mn nuclei were calculated from the observed hyperfine heat capacities by neglecting the contributions from Cu nuclei. These values and that of γ-manganese give a more or less linear relation between manganese content and H_e, which changes from 65 kOe for γ-manganese to about 305 kOe for the dilute manganese alloys.

I. SOME MEASUREMENTS OF MAGNETIC HYPERFINE HEAT CAPACITIES

A. INTRODUCTION

1. Hyperfine Fields in Magnetically-Ordered Metals and Alloys.

Hyperfine or effective magnetic fields H_e acting on the nuclei have been observed for a wide variety of magnetic materials.[1] These fields are intimately related to and involved with some of the most fundamental and least understood properties of the electronic structure. Several mechanisms have been proposed to explain their origin. In free ions, neutral atoms and salts of the iron series, the dominant contribution arises from the Fermi contact interaction[2] between the nucleus and the spin or exchange-polarized core electronics.[1,3] It was first pointed out by Sternheimer[4] that for systems with unpaired outer electrons the interaction of these unpaired electrons with electrons of the core would depend on the spin and could produce different spatial distributions for paired core electrons with different spins. With such a polarization, there could then be a difference in the electron density at the nucleus between electrons with opposite spins for all the paired s electrons in the atom. In magnetically-ordered metals and alloys, however, the situation is more complicated since one can not separate any particular atom or nucleus from its complex environment. According to the pioneering paper of Marshall[5] and further investigations of other workers,[1,6,7] mainly related to the iron series, the various contributions to H_e in these substances can be summarized as in the following terms:

i. Local field--this is the usual internal field which includes the external field, the demagnetizing field, the Lorentz field, and any small residue of the local field that exists for non-cubic symmetry.

ii. Core electron field--three different types of core electron contributions are:

(a) The field, via Fermi contact interaction, from core s electrons polarized by unpaired 3d electrons.

(b) The field from any unquenched orbital moment of the 3d electrons.

(c) The dipole field associated with the spin of the 3d electrons. This term is zero for cubic symmetry.

iii. Conduction electron field--a net spin density of the outer s conduction electrons at the nucleus will contribute to H_e via the Fermi contact interaction. This net spin density can arise from the following mechanisms:

(a) Polarization of the conduction electrons by the unpaired 3d electrons in the same way as the core s electrons.

(b) Admixture of conduction electrons into the 3d band.

(c) The covalent mixing of the conduction electrons and 3d electrons of neighbouring ions.

Some of the terms mentioned above give positive field contributions at the nucleus, i.e., the field is parallel to the net spin of the atom, while other terms give negative ones. Therefore the observed hyperfine field is actually a net resultant of terms of opposite signs. In practice, there are still too many uncertainties in theoretical calculation of most of these terms, and more experimental data on hyperfine fields would be valuable as a guide to further theoretical work.

Historically, early precise studies of the optical spectra of free atoms were used to detect the hyperfine interaction of nuclear magnetic moments with the spin and orbital moments of the atomic electrons.

Later the development of microwave techniques made it possible to study this effect in solids by electron paramagnetic resonance. EPR, however, can be observed only in the absence of broadening due to the dipolar field of neighbouring magnetic ions. The dipolar field must therefore either be negligible, as in magnetically dilute substances, or it must be averaged to zero by rapid exchange among the surrounding dipoles. In contrast, the expected splitting of the nuclear energy levels in a solid can only be measured in a magnetically-ordered lattice. Otherwise the electron-lattice relaxation, which is rapid compared with the nuclear Larmor frequency in the field H_e, will give zero $\langle H_e \rangle$.

So far all the experimental data on H_e for magnetically-ordered metals and alloys have been obtained by four different methods, namely, nuclear magnetic resonance, Mössbauer effect, nuclear polarization, and low temperature heat capacity measurements. The first two are spectroscopic in nature, whereas the other two are based on the temperature dependence of the distribution among the various nuclear spin orientation levels in these substances. All of them are complementary, each has advantages but also limitations in certain respects. The two spectroscopic methods are more accurate, provided that hyperfine structures can be well-resolved. Such resolution is not always attainable. They can also be used at a wide range of temperatures to study the temperature dependence of the hyperfine field. The Mössbauer effect method can only be applied to a limited number of nuclei showing this effect. The wider applicability of the nuclear polarization method is a distinct advantage. However, this method and, in some cases, the Mössbauer effect give the product of H_e and the magnetic moment for a nuclear excited state, which is not always known. On the contrary, the interpretation of the results of the heat

capacity method needs only the knowledge of the magnetic moment for the nuclear ground state. The nuclear polarization and the heat capacity measurements have to be performed at low temperatures of the order of $\mu H_e/k$ (μ is the nuclear magnetic moment and k is Boltzmann's constant), and measure only certain average values, not the distribution, of the hyperfine field. Other limitations for the heat capacity method will be discussed in the next section.

Part I of this dissertation presents the results of calorimetric determinations of H_e for several metals and alloys including (a) γ-manganese and chromium, (b) gold-manganese, and (c) dilute osmium and platinum in iron.

For the ferromagnetic metals iron,[8] cobalt,[9-11] and nickel,[12] the values of H_e are known. Since further progress toward understanding the origin of H_e seems to require its evaluation in a variety of situations, the values of H_e for the antiferromagnets of the iron series, α- and γ-manganese and chromium are of interest. However, α-manganese is not suitable for calorimetric measurements because it has four magnetic sites with different moments[13] and presumably different values of H_e. It also has a complicated structure which would make an interpretation of the H_e values difficult, even if they could be measured separately and assigned to the correct sites. The gold-manganese alloy is another antiferromagnetic metal with a relatively simple structure.

The general behavior of the conduction electron contribution to H_e is not well understood. More information on this point, particularly from a systematic study of the hyperfine field at the nuclei of diamagnetic impurities dissolved in magnetically-ordered metals, would help in the interpretation of the magnetic ordering process. H_e values for osmium

and platinum in iron are of interest for comparison with the known H_e values for most of the other third-transition-group elements, all in dilute solution in iron.

2. Magnetic Hyperfine Contribution to Low Temperature Heat Capacity.

The low temperature heat capacity of a normal metallic solid is usually composed of lattice and electronic terms, which relate to the Debye characteristic temperature and the density of states at the Fermi surface of the solid, respectively. In addition to these two terms, however, additional heat capacity terms occur in certain cases due to the occupation of other energy states. The temperature at which such an excess heat capacity will make its appearance and the form of the anomaly depend on the nature of the process involved. By investigating these anomalies one can often obtain information about the energy levels giving rise to them.

One such anomaly arises from the magnetic hyperfine interaction. In the presence of the hyperfine field H_e the spatial degeneracy of the nuclear spin I is removed and each nuclear level is split into its $(2I + 1)$ components. The energy shift of the sub-state with quantum number m is

$$E_m = - \frac{m}{I} \mu H_e \qquad (1)$$

where $m = -I, -I+1, \ldots, I-1, I$ and the direction of H_e has been taken as the axis of quantization. The relative population of these $(2I + 1)$ sub-states changes with temperature. For a system of N atoms the total energy associated with this kind of excitation is

$$E_N = N \frac{\sum_{m=-I}^{m=I} -\frac{m}{I}\mu H_e e^{\frac{m}{I}\left(\frac{\mu H_e}{kT}\right)}}{\sum_{m=-I}^{m=I} e^{\frac{m}{I}\left(\frac{\mu H_e}{kT}\right)}}$$

$$= - N\mu H_e B_I(x) \qquad (2)$$

where $x = \frac{\mu H_e}{kT}$ and the Brillouin function $B_I(x)$ is given by

$$B_I(x) = \frac{2I+1}{2I} \coth\left(\frac{2I+1}{2I}\right)x - \frac{1}{2I} \coth\left(\frac{1}{2I}\right)x \quad . \qquad (3)$$

The additional term in the heat capactiy, which results from increasing the population of the upper states, is obtained by differentiating E_N with respect to the temperature. This leads to a Schottky anomaly

$$\frac{C_N}{R} = -\left(\frac{\mu H_e}{kT}\right)^2 \left[\left(\frac{2I+1}{2I}\right)^2 \operatorname{csch}^2\left(\frac{2I+1}{2I}\right)\left(\frac{\mu H_e}{kT}\right) - \left(\frac{1}{2I}\right)^2 \operatorname{csch}\left(\frac{1}{2I}\right)\left(\frac{\mu H_e}{kT}\right)\right] \qquad (4)$$

where C_N is the heat capacity for Avogadro's number of nuclei and R is the gas constant. For small value of $\left(\frac{\mu H_e}{kT}\right)$ one can use the leading terms in the expansion of Eq. (4) as an approximation

$$\frac{C_N}{R} = \frac{I+1}{3I}\left(\frac{\mu H_e}{kT}\right)^2 - \frac{(2I+1)^4 - 1}{240\ I^4}\left(\frac{\mu H_e}{kT}\right)^4 + \quad .... \qquad (5)$$

The higher order terms are usually negligible in the lowest temperature region practical for heat capacity measurements at the present time.

The above derivation, however, is valid only for a single kind of nuclei in a uniform hyperfine field. As a general expression for a pure metal, Eq. (5) should become

$$\frac{C_N}{R} = \frac{1}{3}\left\langle\frac{I+1}{I}\mu^2\right\rangle\left(\frac{H_e}{kT}\right)^2 - \frac{1}{240}\left\langle\frac{(2I+1)^4 - 1}{I^4}\mu^4\right\rangle\left(\frac{H_e}{kT}\right)^4 \quad .... \qquad (6)$$

where

$$\left\langle \frac{I+1}{I} \mu^2 \right\rangle = \sum_i A_i \frac{I_i+1}{I_i} \mu_i^2 ;$$

and

$$\left\langle \frac{(2I+1)^4-1}{I^4} \mu^4 \right\rangle = \sum_i A_i \frac{(2I_i+1)^4-1}{I_i^4} \mu_i^4$$

with A_i, I_i, and μ_i the fractional natural abundance, the nuclear spin, and the nuclear magnetic moment, respectively, of isotope i of the element. The summation is to be extended over all isotopic species and over all magnetically non-equivalent sites. The H_e value obtained experimentally from the T^{-2} term by calorimetric measurements is actually the root mean square value of the H_e values at all nuclei. Since the hyperfine field is quite sensitive to the local magnetic properties of a lattice, this mean value should be distinguished from that determined by resonance method. The sign of H_e is also undetermined, unless a sufficiently large external field is applied to make an observable change in C_N, i.e. an external field of at least a few percent of H_e, depending on the accuracy of measurements.

The magnetic hyperfine heat capacity for pure iron series metals has been observed only in cobalt by Heer and Erikson[14] and by Arp, Edmonds, and Petersen.[9] This calorimetric determination of H_e would not be suitable for iron or nickel since only small fractions of their nuclei have nonzero spin and they have relatively small magnetic moments.

Since H_e at the nuclei of different components are generally different, Eq. (6) should be further generalized for alloys

$$C_N = \sum_c n_c (C_N)_c \qquad (7)$$

with n_c the atomic fraction of component c in the alloy, $(C_N)_c$ the value calculated from Eq. (6) for component c, and the summation to be extended over all components. One can use the calorimetric method to obtain H_e for one component of an alloy if (i) only one component has a significant contribution to the total C_N; or (ii) H_e values for all components except the one to be determined are already known from measurements using other methods, and their contribution to C_N is not too large compared with that to be studied; or (iii) heat capacity measurements go low enough in temperature to make the T^{-4} term (or even higher order terms) observable, making possible the evaluation of more than one moment of H_e--i.e., $\langle H_e^2 \rangle$, $\langle H_e^4 \rangle$, etc. In fact most of the experimental work on determining H_e for alloys using low temperature calorimetric measurements belong to type (i). That is, the alloys are composed of a solute and a host such as iron or nickel with small or even negligible C_N contribution.

B. EXPERIMENTAL

1. Apparatus.

Two adiabatic demagnetization calorimeters previously set up for experiments below 1°K by Lien[15] and O'Neal,[16] respectively, were first used in this work. Another apparatus shown in Fig. 1 was then designed for further studies. This apparatus is similar to that described by O'Neal.[16] The major changes included a different paramagnetic cooling salt and its arrangement. Figure 2 shows details of the cooling salt part of this apparatus. Chromium potassium sulfate was used instead of copper potassium sulfate in the hope that more cooling capacity and lower temperatures (approximately 0.05°K) could be obtained. A mixture of 150-gram of freshly-prepared chromium potassium sulfate crystals and 25-gram Apiezon N grease was sucked into a bakelite cage through the side holes. Thermal conduction within the salt was provided by 200 3.75 in. long X 0.025 in. diam gold-plated copper wires with one end of each fastened to a bakelite plate with epoxy-resin and the other end hard-soldered to a copper plate. The latter was in turn thermally attached with Apiezon N grease to the bottom of a copper shield, inside which the sample was rigidly supported with cotton threads. The bakelite cage and the bakelite plate were used to reduce the eddy current heating induced during the demagnetization process. The cage was then rigidly supported at the bottom of a 16.5 in. long X 2.5 in. O.D. X 0.016 in. wall stainless steel tube. This tube provided a high thermal resistance between the cooling salt and the bath. To make this thermal isolation more effective, many slots were made on the tube to a point where the heat leak through it was greatly reduced, but still no appreciable amount of heat due to vibration was produced. For a typical run, the

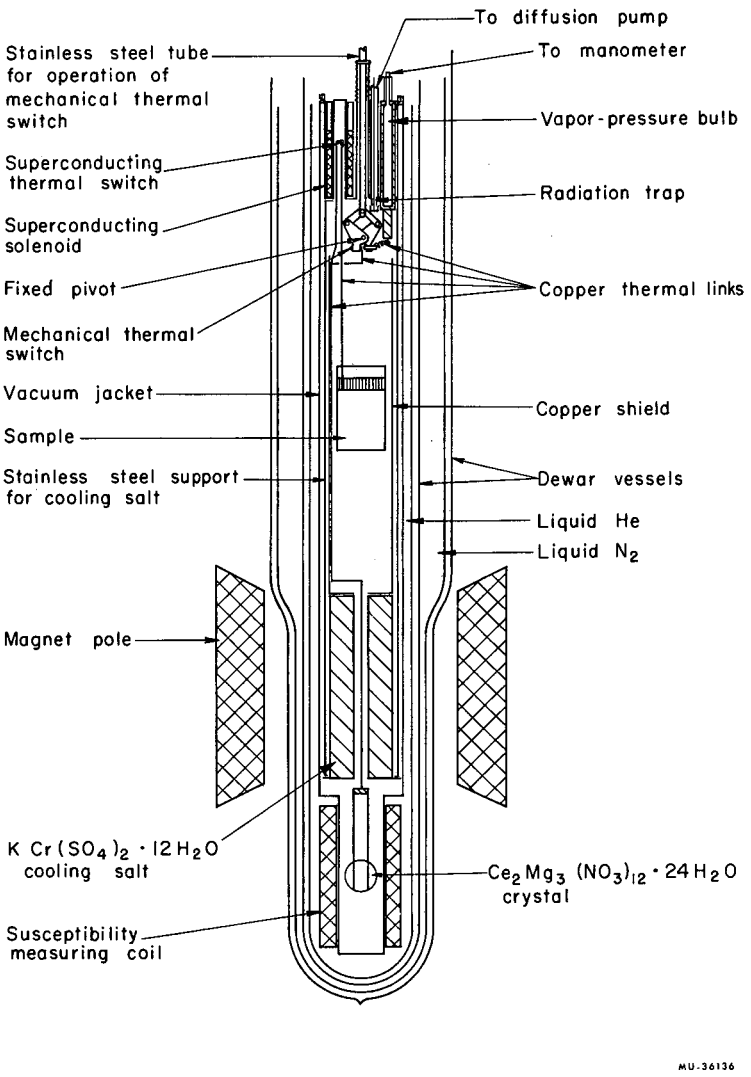
To diffusion pump
To manometer
Stainless steel tube for operation of mechanical thermal switch
Vapor-pressure bulb
Superconducting thermal switch
Radiation trap
Superconducting solenoid
Fixed pivot
Copper thermal links
Mechanical thermal switch
Vacuum jacket
Copper shield
Sample
Stainless steel support for cooling salt
Dewar vessels
Liquid He
Liquid N_2
Magnet pole
$K\,Cr(SO_4)_2 \cdot 12H_2O$ cooling salt
$Ce_2Mg_3(NO_3)_{12} \cdot 24H_2O$ crystal
Susceptibility measuring coil
MU-36136

Fig. 1

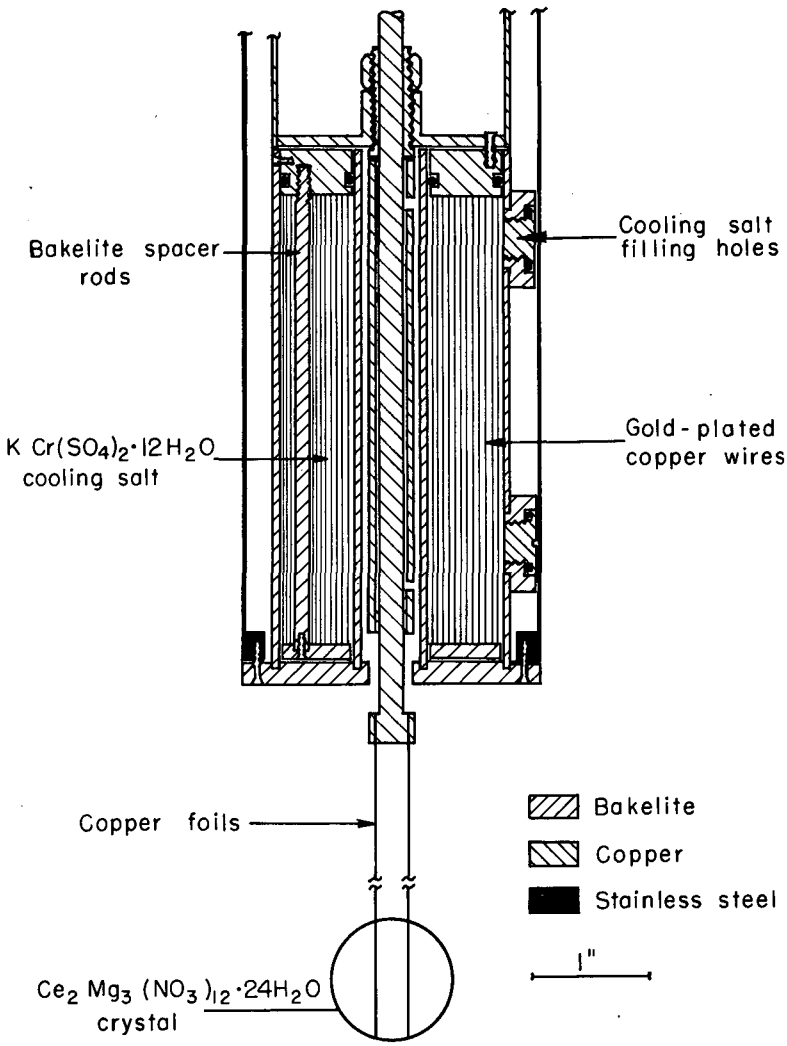
Bakelite spacer rods
Cooling salt filling holes
K Cr(SO4)2·12H2O cooling salt
Gold-plated copper wires
Copper foils
Bakelite
Copper
Stainless steel
1"
Ce2 Mg3 (NO3)12·24H2O crystal
MU-36135

Fig. 2

total heat leak to the cooling salt at 0.05°K was of the order of 500 ergs/min.

The isothermal magnetization process (for removing the large entropy of the paramagnetic cooling salt in zero field at 1°K) was carried out using a 16 KG D.C. magnet and a mechanical heat switch to connect the salt to the 1°K helium bath. The switch, which could be opened later for adiabatic demagnetization, was operated by an air cylinder. The effectiveness of this design has been discussed by Senozan.[17] The superconducting switch was a 2.5 in. long X 0.012 in. diam lead wire controlled by a niobium solenoid.

Three different kinds of thermometers were used for temperature measurements. They were based on the temperature dependence of the pressure over a small amount of helium condensed in a vapor pressure bulb, the magnetic susceptibility of a $Ce_2Mg_3(NO_3)_{12}\cdot 24H_2O$ crystal, and the electrical resistance of an Aquadag or a Speer resistor, respectively. The magnetic thermometer was made by cementing four plate-like single crystals together and cutting to a spherical shape. The plates were then separated and re-cemented (with GE 7031 varnish) with two sheets of copper foil sandwiched in the outer two joints. The tops of the copper foils were then bolted, with Apiezon N grease as the thermal binding agent, to a copper rod which served as the thermal link between the magnetic thermometer and the sample. The advantage of the Speer resistor over the Aquadag was its better reproducibility of R-T characteristics from run to run. A grade-1002-1/2W Speer resistor with nominal resistance of 220 ohms (the actual resistance was higher, since part of the carbon surface was ground off when the outer insulating layer was removed) was repeatedly used in several experiments. It was 500 ohms at 4.2°K,

900 ohms at 1°K, and 9000 ohms at 0.1°K. Below 0.1°K the current dependence of resistance became appreciable. It is believed that this was due to the overheating of the thermometer. However, experience showed that, as long as both the calibration of the thermometer and the heat capacity measurements were made using the same current (about 0.5 μamp), the existence of the steady state temperature difference between sample and thermometer was not serious as far as the heat capacity results were concerned.

For most cases the heater was directly attached to the sample to avoid the use of a separate calorimeter which might make a large contribution to the total measured heat capacity and which might also be in relatively poor thermal contact with the sample. Constantan and manganin wire are commonly used in the construction of heaters for calorimetric measurements. However, we found a tungsten-platinum alloy wire more convenient for this purpose (see Appendix).

For measurements at liquid helium temperatures, the cooling salt, the magnetic thermometer, and the superconducting thermal switch were all removed. The sample was rigidly supported by cotton threads inside a brass cage, which replaced the stainless steel tube. Thermal contact between the sample and the vapor pressure bulb was made directly through the mechanical switch.

2. Procedures.

At the beginning of an experiment the apparatus was first cooled from room temperature to 78°K using hydrogen exchange gas. Liquid hydrogen was then put into the inner (helium) dewar to cool the apparatus to about 14°K. Before liquid helium was transferred into the dewar, the

remaining liquid hydrogen was boiled out with an induction heater and the exchange gas was evacuated by an oil diffusion pump to a pressure of the order of 10^{-6} mm Hg, as measured with an untrapped ionization gauge at room temperature. It took several hours for the sample to cool to 4.2°K with the mechanical thermal switch closed.

The susceptibility of the magnetic thermometer was calibrated against the vapor pressure of liquid helium at about eight temperatures between 4.2 and 1.1°K. The χ-T relation followed a Curie-law and was used as the basis for temperature measurements below 1.1°K. The cooling salt was then magnetized at 1.1°K. It required almost three hours for the heat of magnetization to be conducted away. The mechanical switch was opened and the salt was demagnetized. After the demagnetization process, which took about 30 minutes, was completed constant thermal drifts were obtained in about 10 minutes. With the superconducting switch closed the carbon resistance thermometer (attached directly to the sample) was calibrated against the susceptibility of the magnetic thermometer at about thirty points between the lowest temperature and 1.2°K. Between successive calibration points the temperature of the system was raised by supplying power to a heater attached to the copper shield. The time for establishing thermal equilibrium between the sample thermometer and the magnetic thermometer dependedon the heat capacity of the sample, ranging from about one minute for samples such as copper to almost 20 minutes for samples with large hyperfine heat capacities. The two-salt system[16] enabled us to have a good thermal equilibrium between the two thermometers, even though temperature inhomogeneities still existed within the cooling salt. The temperature-resistance calibration points were then fitted to an equation of the form

$$\frac{1}{T} = C_o + C_1 R + C_2 R^2 + C_3 R^3 + C_4 R^4 + C_5 R^5 \quad (8)$$

The fractional difference between the observed temperature and the calculated temperature from the above equation was plotted against the calculated temperature, and a smooth curve, called the "difference plot", was drawn through the points. This plot was used to correct those temperatures calculated from the equation for heat capacity points.

Following a second demagnetization, the superconducting switch was opened to thermally isolate the sample. Heat capacity points were taken over intervals of T/10 or less. The heat input for each point was determined by passing a measured current through a measured resistance for a measured period of time. The temperature increment was determined by extrapolating the initial and the final drifts of heating curves on the recorder chart to the middle of the heating period.

Measurements at liquid helium temperatures were made with the mechanical switch providing thermal contact between the sample and the vapor pressure bulb. The resistance thermometer was calibrated directly against the vapor pressure of liquid helium at about twenty-five points between 4.2 and 1.1°K.

3. Heat Capacity of Copper.

Heat capacity measurements below 1°K on copper were undertaken to check the new calorimeter. Copper was a good choice for this purpose, since both the T^3 and T terms in its heat capacity were already well determined from previous measurements between 1.0 and 4.2°K where the thermodynamic temperature scale is well established, and there is no reason to expect deviation from the extrapolation to temperatures of interest here.

Two different samples used here included a 140 gram single crystal of 99.9999% pure copper (Sample A) and a 900 gram polycrystalline one of 99.999% pure copper (Sample B). These samples had been used before for heat capacity measurements by Shen[18] (Sample A, 0.3 to 25°K) and Phillips[19] (Sample B, 0.1 to 4.2°K).

The experimental results, after being corrected by subtracting the contributions of the "addenda" to the measured heat capacities, are listed in Table I. Errors associated with addenda corrections and also with the temperature determination have been discussed by O'Neal.[16]

As shown in Fig. 3, the data for both samples fit the equation

$$C(\text{mJ mole}^{-1}\ \text{deg}^{-1}) = 0.0480T^3 + 0.696T \qquad (9)$$

within 1% above 0.1°K and 1.5% below 0.1°K. Since the T^3 term is relatively small in this temperature region, the coefficient used is that determined by Phillips.[19] The T term is in good agreement with that obtained by Shen[18] and Phillips.[19]

It should be pointed out that the lowest temperature for heat capacity measurements was actually limited by the fact that the sample was warmed up by eddy current heating, from an even lower temperature obtained after demagnetization, when the superconducting switch was turned off.

Table I. Heat capacity of copper

T (°K)	C (mJ/mole-deg)	T (°K)	C (mJ/mole-deg)
Sample A:		0.5622	0.3969
0.1166	0.08190	0.6203	0.4429
0.1378	0.09643	0.6959	0.4993
0.1540	0.1073	0.8037	0.5848
0.1640	0.1138	0.9134	0.6742
0.1815	0.1258	0.3920	0.2752
0.1988	0.1383	0.4536	0.3194
0.2163	0.1503	0.6141	0.4382
0.2400	0.1666	0.6983	0.5028
0.2715	0.1892	0.7654	0.5523
0.2962	0.2066	0.8245	0.6008
0.3364	0.2362	0.8930	0.6588
0.1385	0.09689	1.008	0.7553
0.1597	0.1111		
0.1736	0.1208	Sample B:	
0.1914	0.1325	0.07221	0.04961
0.2160	0.1493	0.08344	0.05739
0.2322	0.1625	0.09335	0.06528
0.2530	0.1752	0.1079	0.07637
0.2926	0.2033	0.1210	0.08540
0.3133	0.2173	0.1316	0.09050
0.3404	0.2392	0.1420	0.09912
0.1598	0.1111	0.1537	0.1075
0.1848	0.1284	0.07138	0.04869
0.2209	0.1531	0.09113	0.06427
0.2556	0.1786	0.1014	0.07109
0.2973	0.2084	0.1114	0.07778
0.3447	0.2401	0.1211	0.08453
0.3906	0.2746	0.1349	0.09304
0.4524	0.3187	0.1466	0.1016
0.5057	0.3578	0.1604	0.1118

Table I. (Continued)

T (°K)	C (mJ/mole-deg)	T (°K)	C (mJ/mole-deg)
0.1778	0.1235	1.125	0.8590
0.1968	0.1368	0.2084	0.1448
0.2167	0.1507	0.2302	0.1604
0.2367	0.1648	0.2517	0.1761
0.2586	0.1794	0.2754	0.1919
0.2832	0.1984	0.3018	0.2105
0.3121	0.2175	0.3315	0.2325
0.3428	0.2412	0.3670	0.2594
0.4209	0.2982	0.4097	0.2899
0.4590	0.3254	0.4712	0.3321
0.4995	0.3533	0.5132	0.3632
0.5461	0.3875	0.5678	0.4050
0.5947	0.4217	0.6243	0.4473
0.6408	0.4563	0.6794	0.4859
0.6992	0.5033	0.7416	0.5349
0.7619	0.5531	0.8113	0.5930
0.8298	0.6079	0.8780	0.6436
0.9175	0.6776	0.9541	0.7087
1.012	0.7634	1.034	0.7752

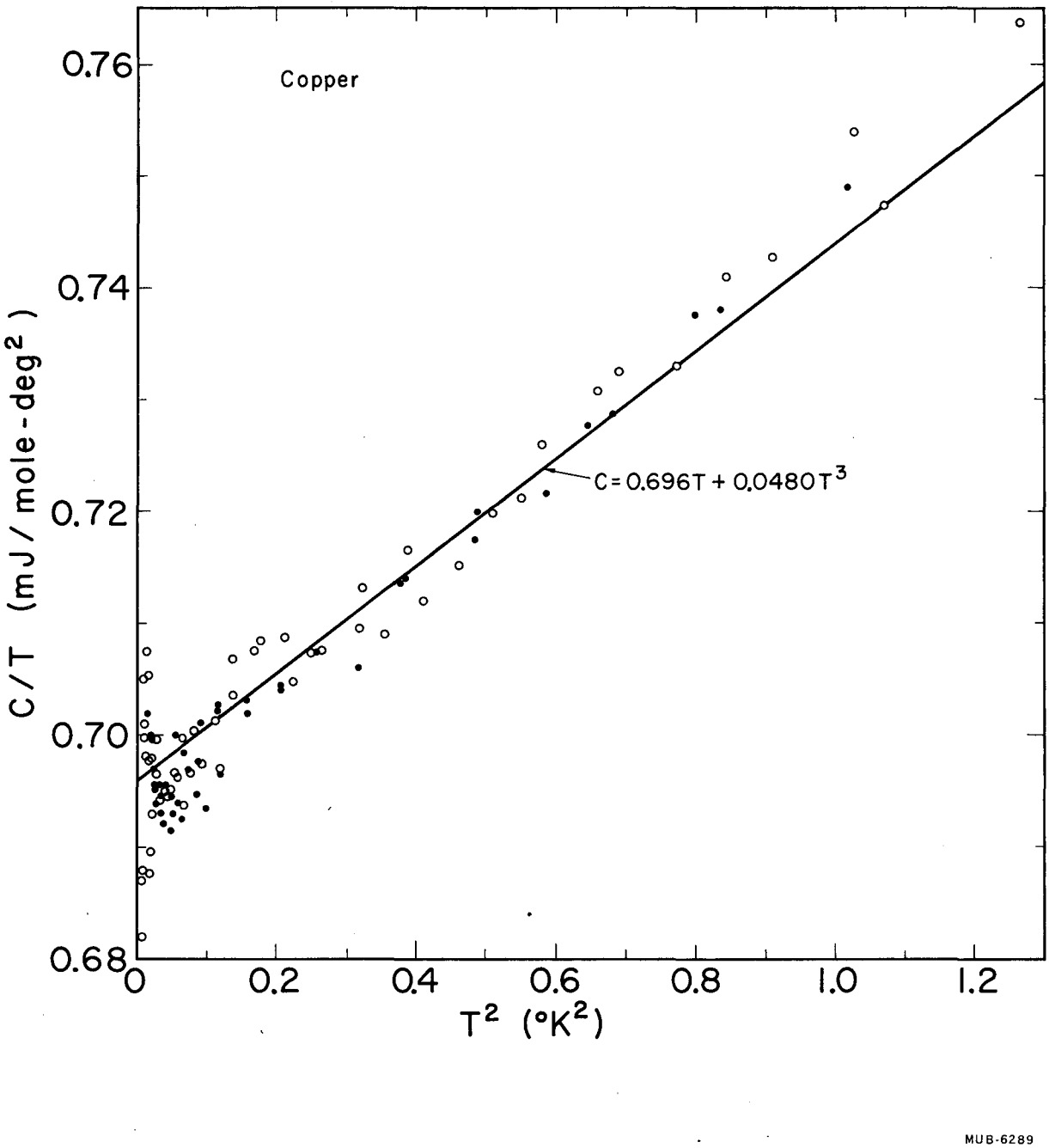
Copper
C = 0.696T + 0.0480T³
C/T (mJ / mole-deg²)
T² (°K²)
0.76
0.74
0.72
0.70
0.68
0
0.2
0.4
0.6
0.8
1.0
1.2
MUB-6289

Fig. 3

C. RESULTS AND DISCUSSION

1. γ-Manganese and Chromium

The γ-manganese crystal is face-centered tetragonal[20] with c = 3.54Å and c/a = 0.94.[21] Below a Néel temperature of 660°K, ions with n_{eff} = 2.4 Bohr magnetons are aligned parallel to the c-axis to produce a magnetic structure in which each ion has eight antiparallel nearest neighbours and four parallel neighbours at a slightly greater distance.[22,23]

The sheet-like sample (0.007 in. thick) was prepared by electrolytic deposition under conditions known to produce the γ-phase[24] and the absence of α-phase material was confirmed by X-ray examination both before and after the heat capacity measurements. Ten such sheets (1 in. by 2 in.) with a total weight of 16.3 gr were stuck together with GE 7031 varnish. As shown in Fig. 4, the experimental points over the range 0.066 to 4.2°K fit the equation

$$C(\text{mJ mole}^{-1}\ \text{deg}^{-1}) = 0.055T^3+9.20T+0.264T^{-2}. \qquad (10)$$

The electronic heat capacity is somewhat higher than that determined by Shinozaki et al.[25] Using the values, A = 100%, I = 5/2, and μ = 3.4614 nm for Mn^{55},[26] an $|H_e|$ of 65 kOe is obtained by comparison of the observed T^{-2} term and Eq. (5). The overestimate of $|H_e|$ arising from the neglect of electric quadrupole splittings, which also gives a T^{-2} term as the high temperature tail in the heat capacity, is shown to be less than 8% by the absence of a measurable T^{-3} term in the observed heat capacity, and comparison with other metals suggests that it is not significant. For example, if the electric field gradient in γ-manganese is of the same order as it is in indium (which is also face-centered tetragonal and has a nuclear quadrupole heat capacity previously determined by O'Neal),[16] the expected T^{-2}

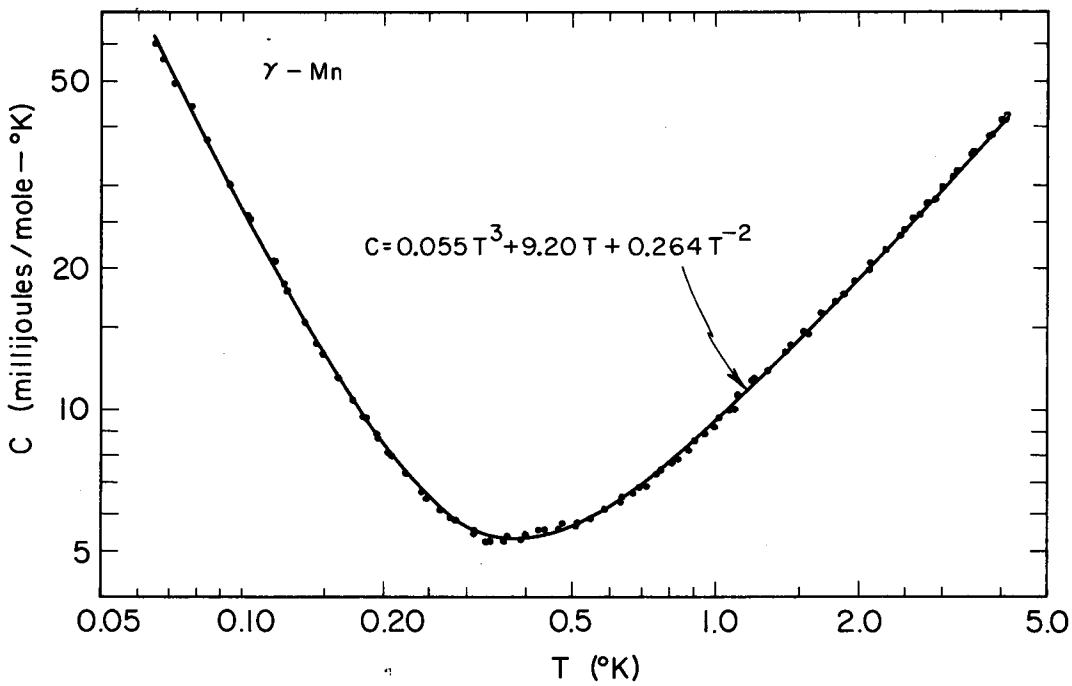
γ – Mn
C=0.055T³+9.20T+0.264T⁻²
C (millijoules/mole – °K)
50
20
10
5
0.05
0.10
0.20
0.5
1.0
2.0
5.0
T (°K)
MU-32838

Fig. 4

term associated with electric quadrupole splittings is only one tenth of one percent of the observed T^{-2} term. By neglecting the slight tetragonal distortion and using sums of dipole fields for cubic arrays,[27] the dipole field H_{dipole} is estimated to be -7.7 kOe. Since this experiment determines only $|H_e|$, this gives $H_e - H_{dipole} = -57$ or 73 kOe.

It is interesting to point out here that the value of H_e for the antiferromagnetic α-manganese has recently been determined calorimetrically to be 90 and 100 kOe by Scurlock et al.[28] and Stetsenko et al.,[29] respectively. However, the crystal structure of α-manganese is complex, the unit cell containing 58 atoms distributed among four non-equivalent sites.[30] Ions at each of these sites have different electronic magnetic moments[13] and their nuclei will experience different hyperfine fields and also will see different dipole fields. Thus the value of H_e deduced from the heat capacity measurements is the root mean square of the fields at all nuclei in the four different sites weighted according to their abundances. We have tried to make a further analysis of the result of Scurlock et al.[28] by assuming that the ratio of H_e to n_{eff} is constant for all sites. Kasper et al.[13] could not assign unambiguous magnetic moments to the various sites in α-manganese, but they did propose two models that were consistent with their neutron diffraction measurements: Model A with $1.54\mu_B$ at the 2 type I site atoms, $1.54\mu_B$ at the 8 type II site atoms, $3.08\ \mu_B$ at the 24 type III site atoms, and 0 at the 24 type IV site atoms; and model B with $2.50\mu_B$ at the 2 type I site atoms, $2.50\mu_B$ at the 8 type II site atoms, $1.70\mu_B$ at the 24 type III site atoms, and 0 at the 24 type IV site atoms. On this basis, we obtain $H_e/n_{eff} = 44$ kOe/μ_B for Model A and 60 kOe/μ_B for Model B, as compared with 27 kOe/μ_B for γ-manganese. Itoh et al.[31]

in their NMR experiment on α-manganese found a small hyperfine field of the order of 13 kOe and suggested that it might arise from Mn nuclei at magnetic site IV, on which site a moment is absent or, it it exists, is very small. (If it is true, our calculation mentioned above should be corrected, but only by a few percent.)

The chromium crystal is body-centered cubic and has a Néel temperature near 310°K.[32] A long range modulation of the antiferromagnetic moment distribution was observed and interpreted in terms of an antiphase antiferromagnetic domain structure by Corliss et al.[32] and Bacon.[33] Later investigation by Shirane et al.[34] strongly suggested another ordered moment arrangement in which the magnitudes of the magnetic moments are sinusoidally modulated. They give a maximum Bohr magnetron number of 0.59 but an average of 0.46, which is in good agreement with the value for all moments deduced from the antiphase model. In either case the hyperfine field at the nuclei is expected to be rather small. Furthermore, for natural chromium, only 9.55% Cr^{53} has nonzero nuclear spin ($I = 3/2$) and also a small nuclear magnetic moment $\mu = -0.47354$ nm.[26] Therefore, even with the smallest electronic heat capacity among the iron series metals, the magnetic hyperfine heat capacity might be still only a very small fraction of the total heat capacity at 0.06°K (the lowest temperature at which we have been able to make measurements) and therefore difficult to separate from the dominant electronic contribution.

Two high purity metallic chromium samples, both produced at the Albany, Oregon Station of the Bureau of Mines, were prepared by hydrogen purification of electrolytic chromium, followed by arc melting under helium atmosphere. Sample A was a cylinder weighing 480 gr.

Sample B, with a total weight of 280 gr., was composed of five plate-like pieces held together through a central hole by a high purity copper bolt. G.E. 7031 varnish was applied between finished surfaces of each piece to provide a good thermal contact.

The experimental data for both samples are listed in Table 4. Using the lattice heat capacity value determined by Rayne and Kemp[35] from measurements in the liquid-helium temperatures region, a plot of $(C-0.00778T^3)/T$ versus T, as shown in Fig. 5, gives a straight line parallel to the T-axis. Therefore, we have

$$C(\text{mJ mole}^{-1}\ \text{deg}^{-1}) = 0.00778T^3 + 1.45T. \qquad (11)$$

The electronic heat capacity is in reasonable agreement with that of Rayne and Kemp.[35] The lack of the appearance of the T^{-2} term at temperatures as low as 0.06°K suggests that either the H_e value is too small to be observed or there is a very long nuclear spin-lattice relaxation time, T_1. At 0.06°K the background heat input to the sample prevented observation of thermal drifts following heat capacity points for more than one minute. At this temperature, therefore, we can only conclude that either $T_1 > 1$ min or $C_N \leq 0.002$ mJ/mole-deg (based on the scatter of points in Fig. 5 and possible errors associated with the temperature scale), which corresponds to $H_e \leq 7.5$ kOe. At 0.1°K the heat leak from the sample to the cooling salt system balanced the background heat input, and longer thermal drifts, up to 20 minutes, could be obtained. The linearity of the drifts suggests that, at 0.1°K, either $T_1 > 20$ min or $C_N \leq 0.002$ mJ/mole-deg, which now gives $H_e \leq 13$ kOe.

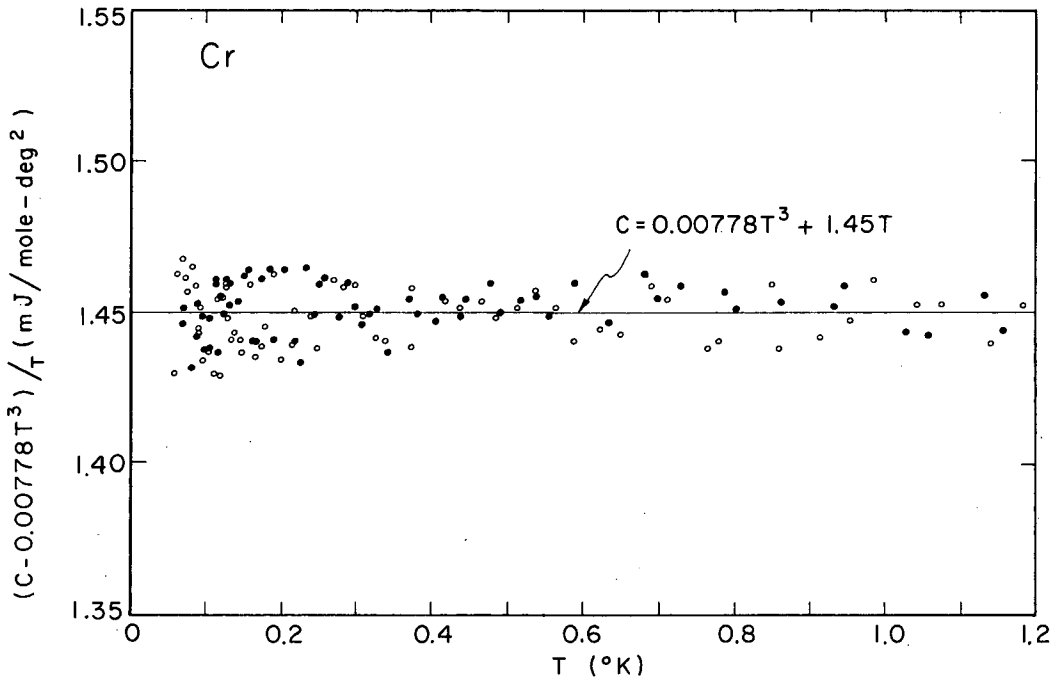
Cr
C = 0.00778T³ + 1.45T
(C - 0.00778T³) / T (mJ/mole - deg²)
T (°K)
1.55
1.50
1.45
1.40
1.35
0
0.2
0.4
0.6
0.8
1.0
1.2
MU-36581

Fig. 5

However, $T_1 \geq 20$ min at 0.1°K seems unlikely as compared with the T_1 values for other metals of the iron series, iron, cobalt, nickel,[36] and α-manganese.[31] This leads to the conclusion that the H_e value for chromium has an upper limit of 13 kOe.

Recently Stetsenko and Avksent'ev[29] reported that they had found an H_e of 150 kOe for chromium. We believe that the observed T^{-2} term in their calorimetric measurements must be associated with an impurity effect or other experimental errors.

In Table 2 the H_e value for γ-manganese and the upper limit of H_e for chromium are compared with the corresponding quantities for iron, cobalt, and nickel. In iron, cobalt, and nickel, the major contribution to H_e is the core polarization term, H_c. Calculations by Watson and Freeman,[1] and experimental data on salts of the divalent ions,[3] both suggest the approximate rule $H_c(\text{kOe}) \approx -126\, n_{eff}$ for ions of the first transition group elements. For the ferromagnetic metals this rule gives an H_c close to the observed H_e (see Table 2) and not large enough to compensate for the expected positive contributions. As noted by Watson and Freeman,[1] the agreement between the observed H_e and the calculated H_c may be a consequence of the partial cancellation of the 4s-electron contribution pointed out by Anderson and Clogston.[7] However, it appears that the estimated H_c is more likely to be too small in magnitude than too large. For the antiferromagnetic metals the same rule gives $H_c \approx -300$ kOe for γ-manganese and -57 kOe for chromium, showing that the calculated H_c is too large or that the other contributions are more positive than in the ferromagnetic metals.

It is not clear how the 4s-electron contribution would be affected by the change from ferromagnetic ordering to antiferromagnetic ordering

but it seems possible that it contributes to the apparent difference between γ-manganese and chromium and the ferromagnetic metals. Another effect which might be important is the exchange polarization of the 3s-electrons of one ion by the 3d-electrons of its neighbours. This effect has been noted as a possible source of the hyperfine fields in diamagnetic atoms dissolved in ferromagnets[1] and the sensitivity of the 3s polarization to the 3d spin density in the outer region of the ion[6] and the amplitudes of the Hartree-Fock orbitals at half the nearest neighbour distance suggest that it might be significant in the pure metals. In a ferromagnet with net spin ↑ , the 3d ↑ spin density on neighbours may tend to counteract the inward attraction of the 3s ↑ electrons, making H_c more negative and improving agreement between experiment and theory. In an antiferromagnet the effect of nearest neighbours would be reversed and H_c would be made less negative.

Table II. Observed hyperfine fields H_e and dipole field contribution H_{dipole}. All fields are in kOe. For chromium, γ-manganese, and hcp cobalt the sign of H_e is not determined by the experiments.

Metal	Reference	H_e	H_{dipole}	$H_e - H_{dipole}$	$-126 n_{eff}$
Cr	This work	≤ 13	0	≤ 13	-57
γ-Mn	This work	± 65	-7.7	- 57, + 73	-300
Fe	a	-330	0	-300	-280
Co (hcp)	b	228	~0	228	-217
Co (fcc)	c	-213	0	-213	-217
Ni	d	- 80	0	- 80	- 77

a. S.S. Hanna, J. Heberle, G.J. Perlow, R.S. Preston, and D.H. Vincent, Phys. Rev. Lett. 4, 513 (1960).

b. Y. Koi, A. Tsujimara, T. Hihara, and T. Kushida, J. Phys. Soc. Japan 17, Suppl. B1, 96 (1961).

c. A.C. Gossard and A.M. Portis, Phys. Rev. Lett. 3, 164 (1959).

d. R.L. Streever, Phys. Rev. Lett. 10, 232 (1963).

Table 3. Heat Capacity of γ-Manganese

T (°K)	C (mJ/mole-deg)	T (°K)	C (mJ/mole-deg)
0.06600	60.03	0.5029	5.629
0.06846	55.57	0.5426	5.869
0.07306	49.18	0.5840	6.157
0.07822	43.88	0.6303	6.522
0.08553	37.23	0.6858	6.816
0.09526	29.95	0.7455	7.235
0.1039	25.74	0.8071	7.731
0.1156	20.64	0.8723	8.193
0.1236	18.53	0.9450	8.829
0.1442	13.94	1.023	9.598
0.1047	25.29	1.078	10.04
0.1167	20.70	0.1793	0.764
0.1250	17.79	0.1919	8.895
0.1363	15.43	0.2038	8.120
0.1483	13.16	0.2444	6.539
0.1598	11.74	0.2728	5.881
0.1708	10.51	0.3039	5.507
0.1818	9.613	0.3338	5.246
0.1936	8.720	0.3630	5.399
0.2060	8.010	0.3963	5.410
0.2213	7.334	0.4341	5.549
0.2404	6.695	0.4725	5.728
0.2608	6.117	0.5086	5.742
0.2817	5.802	0.6222	6.387
0.3038	5.473	0.6644	6.621
0.3280	5.247	0.7097	6.881
0.3549	5.247	0.7626	7.439
0.3857	5.280	0.8275	7.942
0.4225	5.512	0.9042	8.579
0.4634	5.589	0.9941	9.204

Table 3. (Continued)

T (°K)	C (mJ/mole-deg)	T (°K)	C (mJ/mole-deg)
1.071	9.940	3.787	38.42
1.123	10.81	4.014	41.15
1.203	11.63	4.140	42.60
1.435	1.380	1.188	11.54
1.552	14.75	1.277	12.11
1.668	15.99	1.402	13.38
1.801	17.09	1.541	14.57
1.957	18.88	1.869	17.84
2.118	20.47	2.089	20.03
2.279	21.99	2.501	24.18
2.445	23.67	2.689	26.08
2.623	25.64	2.905	28.17
2.810	27.57	3.169	31.36
3.014	29.80	3.487	34.98
3.243	32.35	3.838	38.58
3.497	35.21	4.105	41.88

Table 4. Heat Capacity of Chromium

T (°K)	C (mJ/mole-deg)	T (°K)	C (mJ/mole-deg)
Sample A:		0.2258	0.3237
0.07039	0.1018	0.2427	0.3519
0.08358	0.1197	0.2585	0.3778
0.09019	0.1301	0.2905	0.4241
0.09785	0.1417	0.3084	0.4462
0.1054	0.1526	0.3289	0.4775
0.1139	0.1662	0.3841	0.5572
0.1217	0.1771	0.4172	0.6077
0.1319	0.1926	0.2771	0.4015
0.06965	0.1011	0.2965	0.4305
0.09030	0.1312	0.3190	0.4625
0.09821	0.1412	0.3432	0.4934
0.1064	0.1530	0.3729	0.5427
0.1142	0.1667	0.4052	0.5869
0.1227	0.1778	0.4398	0.6376
0.1322	0.1921	0.4777	0.6981
0.1435	0.2086	0.5170	0.7528
0.1545	0.2258	0.5564	0.8078
0.1651	0.2379	0.6368	0.9231
0.1770	0.2585	0.6810	0.9987
0.1896	0.2732	0.7316	1.070
0.2184	0.3147	0.7912	1.157
0.2354	0.3448	0.9470	1.388
0.2543	0.3712	1.058	1.535
0.1200	0.1725	1.157	1.683
0.1284	0.1875	0.4472	0.6511
0.1574	0.2304	0.4908	0.7125
0.1712	0.2464	0.5414	0.7893
0.1866	0.2732	0.5921	0.8661
0.2056	0.3011	0.7003	1.021

Table 4. (continued)

T (°K)	C (mJ/mole-deg)	T (°K)	C (mJ/mole-deg)
0.8041	1.170	0.3743	0.5387
0.8616	1.257	0.4185	0.6089
0.9365	1.367	0.4655	0.6774
1.029	1.493	0.5135	0.7463
1.134	1.662	0.5649	0.8213
		0.6230	0.9018
Sample B:		0.6900	1.009
0.05929	0.08470	0.7670	1.107
0.07175	0.1049	0.8612	1.244
0.06214	0.09090	0.9561	1.391
0.08478	0.1242	1.043	1.523
0.07091	0.1041	1.143	1.658
0.08904	0.1286	0.09385	0.1362
0.09762	0.1400	0.1052	0.1511
0.1082	0.1556	0.1161	0.1689
0.1185	0.1693	0.1258	0.1835
0.07357	0.1072	0.1358	0.1957
0.08585	0.1252	0.1477	0.2128
0.1116	0.1595	0.1598	0.2333
0.1228	0.1786	0.1745	0.2511
0.1371	0.1978	0.1921	0.2810
0.1507	0.2165	0.2140	0.3081
0.1650	0.2368	0.2409	0.3493
0.1796	0.2595	0.2710	0.3960
0.1996	0.2864	0.2983	0.4355
0.2206	0.3201	0.3259	0.4702
0.2477	0.3562	0.3741	0.5457
0.2809	0.4099	0.3463	0.6339
0.3102	0.4496	0.4880	0.7078
0.3403	0.4906	0.5381	0.7852
0.5915	0.8533	0.9119	1.319
0.6498	0.9397	0.9852	1.446
0.7126	1.039	1.076	1.572

Table 4. (continued)

T (°K)	C (mJ/mole-deg)	T (°K)	C (mJ/mole-deg)
0.7794	1.127	1.184	1.733
0.8470	1.241		

2. Gold-Manganese

In order to make a further test for the above observation of hyperfine fields in antiferromagnets, the value of H_e at Mn nuclei in a single crystal sample of gold-manganese alloy near the composition AuMn was measured by calorimetric method. This alloy, with an actual gold content of 51.5 at.%, forms an ordered body-centered tetragonal structure with c = 3.16Å and c/a = 0.97.[37] (In Fig. 6, the magnetic structures of γ-manganese and gold-manganese are shown for comparison.) Mn ions with $n_{eff} \sim 4$ Bohr magnetons are aligned to produce a magnetic structure in which successive ferromagnetic layers in the antiferromagnetic arrangement are perpendicular to the c-axis.[37] Therefore, each Mn ion has two anti-parallel Mn-ion nearest neighbours and four parallel Mn-ion neighbours at a slightly greater distance.

The heat capacity measurements were made between 0.14 and 1.18°K. The data below 0.8°K fit the equation

$$C(\text{mJ mole}^{-1}\ \text{deg}^{-1}) = 1.05T + 3.21T^{-2} - 0.00156T^{-4}. \qquad (12)$$

The T and T^{-2} terms were determined by the slope and intercept of a plot of CT^2 versus T^3 for the temperature region between 0.4 and 0.8°K as shown in Fig. 7, and the T^{-4} term was determined as explained below. Above 0.8°K the lattice heat capacity becomes observable. This contribution is only several percent of the total heat capacity for the highest-temperatures measurements, and it is therefore not possible to determine the coefficient of the T^3 term accurately.

Since Au nuclei have very small magnetic moment[26] ($\mu_{Au}^2/\mu_{Mn}^2 = 0.0015$), the observed hyperfine heat capacity can be considered to come from Mn nuclei only. An $|H_e|$ of 320 kOe at Mn nuclei is thus calculated from the T^{-2} term. (Actually even with an H_e of 2000 kOe at Au nuclei,

γ – Mn

c = 3.54 Å

c/a = 0.94

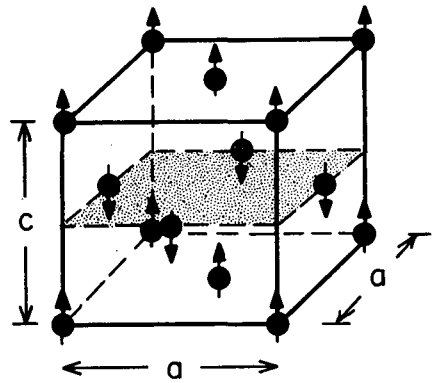

● Mn

○ Au

Au Mu

c = 3.16 Å

c/a = 0.97

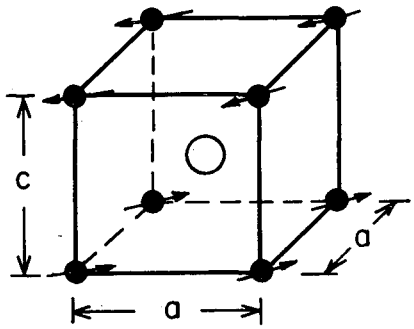

MU-36580

Fig. 6

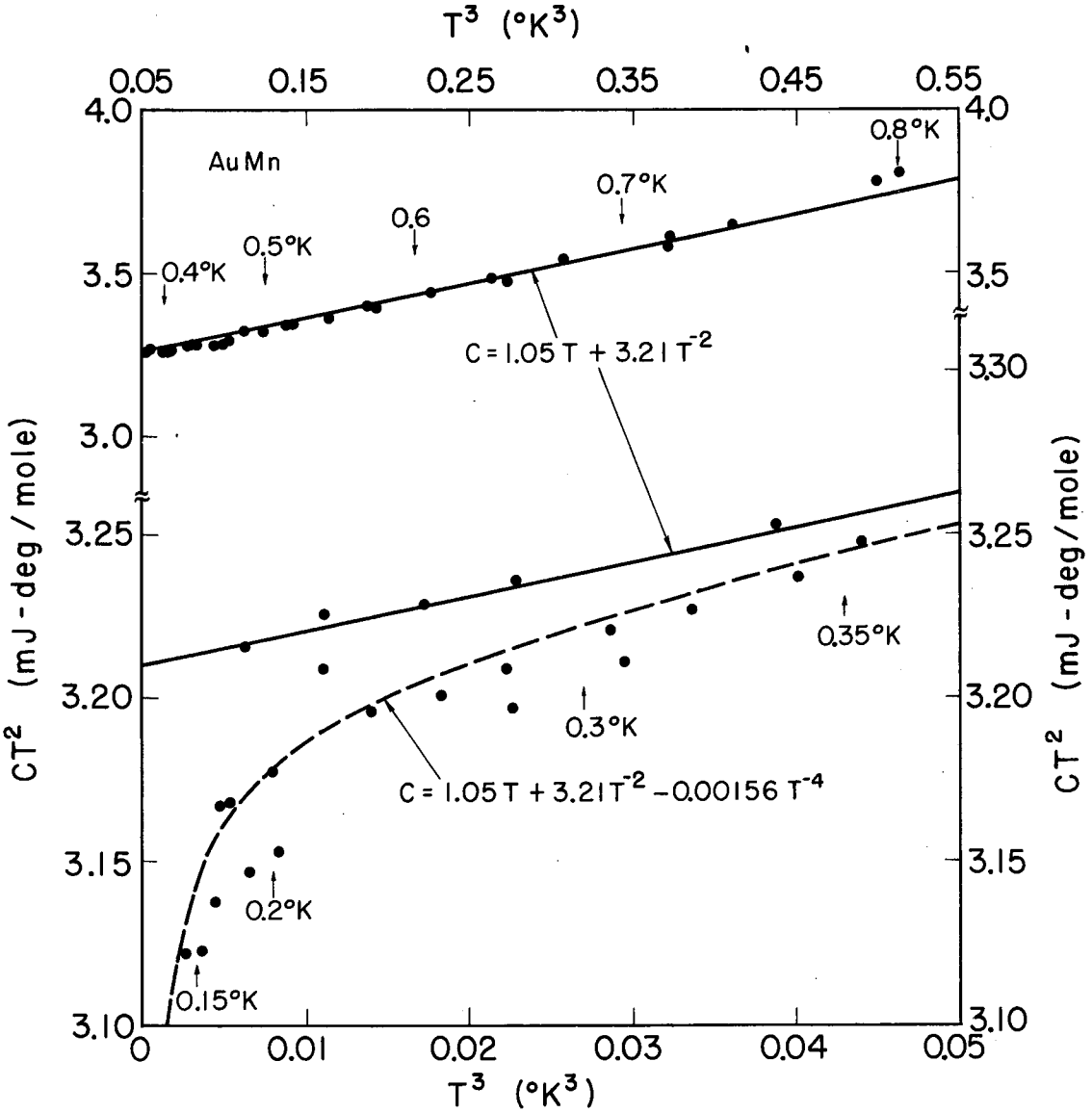
T³ (°K³)
0.05
0.15
0.25
0.35
0.45
0.55
4.0
3.5
3.0
3.25
3.20
3.15
3.10
Au Mn
0.8°K
0.7°K
0.6
0.5°K
0.4°K
C = 1.05 T + 3.21 T⁻²
0.35°K
0.3°K
C = 1.05 T + 3.21 T⁻² − 0.00156 T⁻⁴
0.2°K
0.15°K
CT² (mJ - deg / mole)
3.30
0
0.01
0.02
0.03
0.04
0.05
MUB-6287

Fig. 7

which is presumably a high guess, the contribution from Au nuclei is still only 7.5% of the observed T^{-2} term, and the value of H_e at Mn nuclei drops only from 320 to 308 kOe.) This value is used to calculate the expected T^{-4} term in the heat capacity, which is that given in Eq. 12.

It is clear that again the observed $|H_e|$ at Mn nuclei in this antiferromagnet, as that in γ-manganese and chromium, is smaller than $126n_{eff}$ = 500 kOe. The fact that $|H_e| / 126n_{eff} > 1/2$ as compared with ~1/5 for γ-manganese might well be understood by considering the different numbers and distances of near Mn neighbours. That is, each Mn ion in AuMn has fewer (2) and more remote (3.16Å) nearest Mn neighbours with anti-parallel spins than it does in γ-Mn (8, 2.59Å).

Table 5. Heat Capacity of Gold-Manganese

T (°K)	C (mJ/mole-deg)	T (°K)	C (mJ/mole-deg)
0.2224	64.87	0.5770	10.19
0.2404	55.32	0.6476	8.281
0.2630	46.29	0.7200	6.959
0.2090	37.79	0.7931	6.010
0.3225	31.02	0.8750	5.141
0.3529	26.09	0.9704	4.482
0.3813	22.46	1.047	4.142
0.4080	19.63	1.096	3.915
0.4352	17.31	1.177	3.764
0.4613	15.42	0.1404	158.3
0.4968	13.46	0.1532	133.0
0.5459	11.28	0.1687	111.3
0.6090	9.277	0.1840	94.99
0.6748	7.773	0.2005	80.43
0.7432	6.606	0.2583	48.41
0.8245	5.653	0.2810	40.64
0.8993	4.983	0.3055	34.51
0.9782	4.458	0.3383	28.43
1.026	4.211	0.3698	23.89
1.095	3.952	0.3397	20.39
1.161	3.779	0.4303	17.69
0.2836	40.24	0.4679	15.03
0.3087	33.69	0.5155	12.55
0.3423	27.62	0.5718	10.41
0.3767	22.98	0.6418	8.467
0.4077	19.68	0.7186	6.931
0.4325	17.53	0.8001	5.945
0.4547	15.86	0.9015	4.951
0.4818	14.32	1.000	4.347
0.5211	12.30	1.078	4.027
1.172	3.759	0.1997	79.73
0.1646	115.8	0.2025	76.91
0.1750	103.4	0.2229	64.92
0.1868	90.17		

3. Dilute Osmium and Platinum in Iron

An alloy of iron with 3.21 at.% Pt was prepared by melting 99.999% iron sponge and 99.9% Pt foil chips in a helium atmosphere, and was homogenized by annealing for 20 hours at 1300°C. A sample containing 0.75 at.% Os in iron of the same purity was supplied by Johnson, Matthey and Co., Ltd. The heat capacity of these two alloys have been measured from 0.08 to 1.15°K. The experimental data were analysed by plotting CT^2 versus T^3, as shown in Figs. 8 and 9. The straight-line regions of these plots gave the T^{-2} and T terms in the heat capacities,

$$C(\text{mJ g}^{-1}\text{ deg}^{-1}) = 8.36\times10^{-2}T + 1.12\times10^{-4}T^{-2} \qquad (13)$$

for 0.75 at.% Os in Fe, and

$$C(\text{mJ g}^{-1}\text{ deg}^{-1}) = 8.25\times10^{-2}T + 1.40\times10^{-3}T^{-2} \qquad (14)$$

for 3.21 at.% Pt in Fe. The observed T^{-2} terms were corrected by subtracting the contribution expected for the iron nuclei in pure iron (the corrections were 3.3% and 0.25% for the Os and Pt samples respectively) and were then used to calculate H_e values. The calculation was based on the following data[26] for the isotopic abundances, spins, and nuclear moments: 1.64% Os^{187} with $I = 1/2, \mu = 0.12$nm; 16.1% Os^{189} with $I = 3/2, \mu = 0.6507$nm; 33.8% Pt^{195} with $I = 1/2, \mu = 0.6004$nm. The resulting values of H_e -- 1400 kOe for Os and 1390 kOe for Pt -- were used to calculate the expected T^{-4} terms in the heat capacity. (The contributions of the iron nuclei to the T^{-4} terms are completely negligible.) On this basis, the hyperfine heat capacities of the solute nuclei alone are

$$C(\text{mJ g}^{-1}\text{ deg}^{-1}) = 1.08\times10^{-4}T^{-2} - 4.53\times10^{-8}T^{-4} \qquad (15)$$

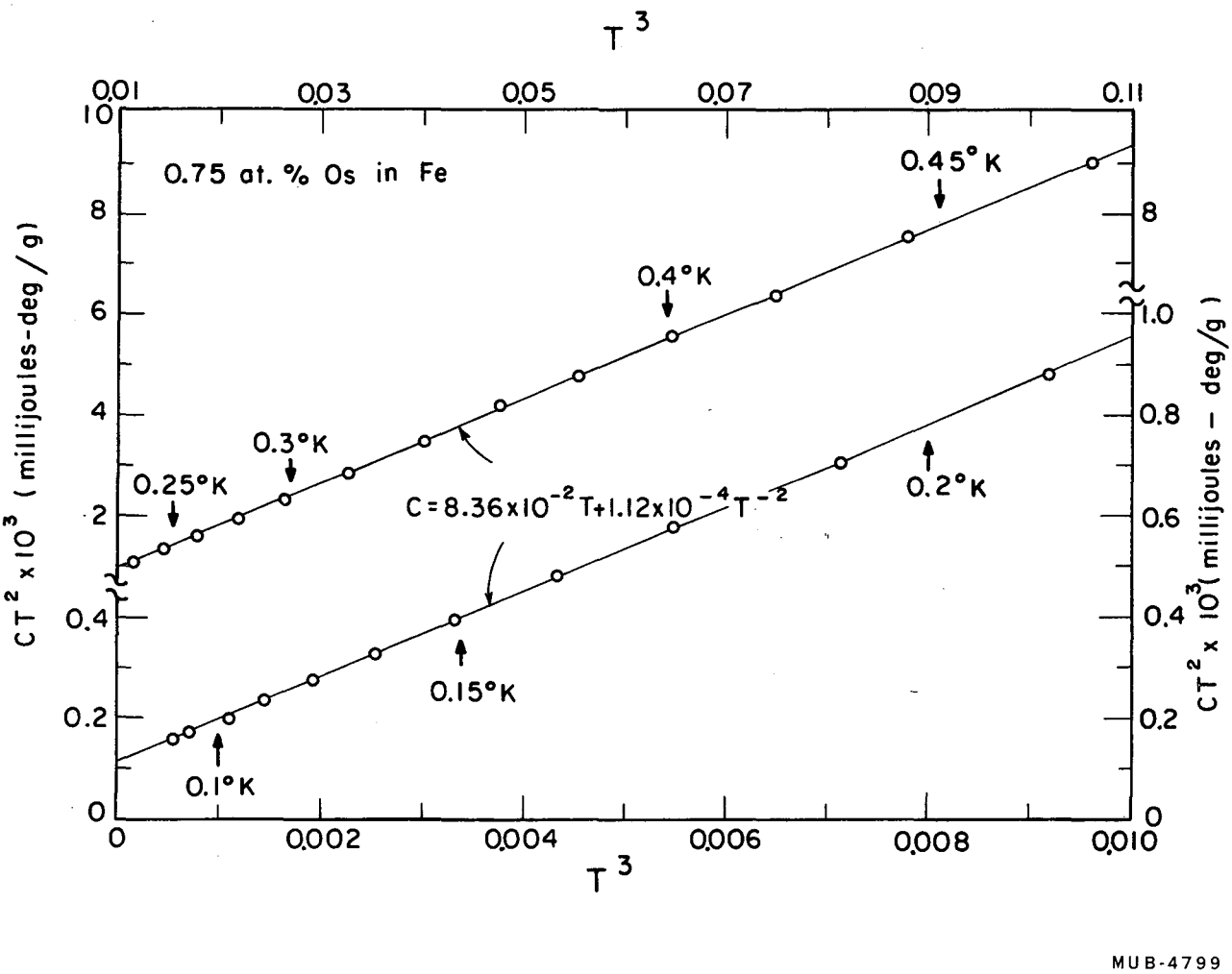
T 3
0.01
0.03
0.05
0.07
0.09
0.11
0.75 at. % Os in Fe
0.45° K
0.4° K
0.3° K
0.25° K
0.2° K
0.15° K
0.1° K
C = 8.36x10-2 T+1.12x10-4 T-2
CT2 x 103 (millijoules-deg/g)
CT2 x 103 (millijoules - deg/g)
0
0.002
0.004
0.006
0.008
0.010
T 3
MUB-4799

Fig. 8

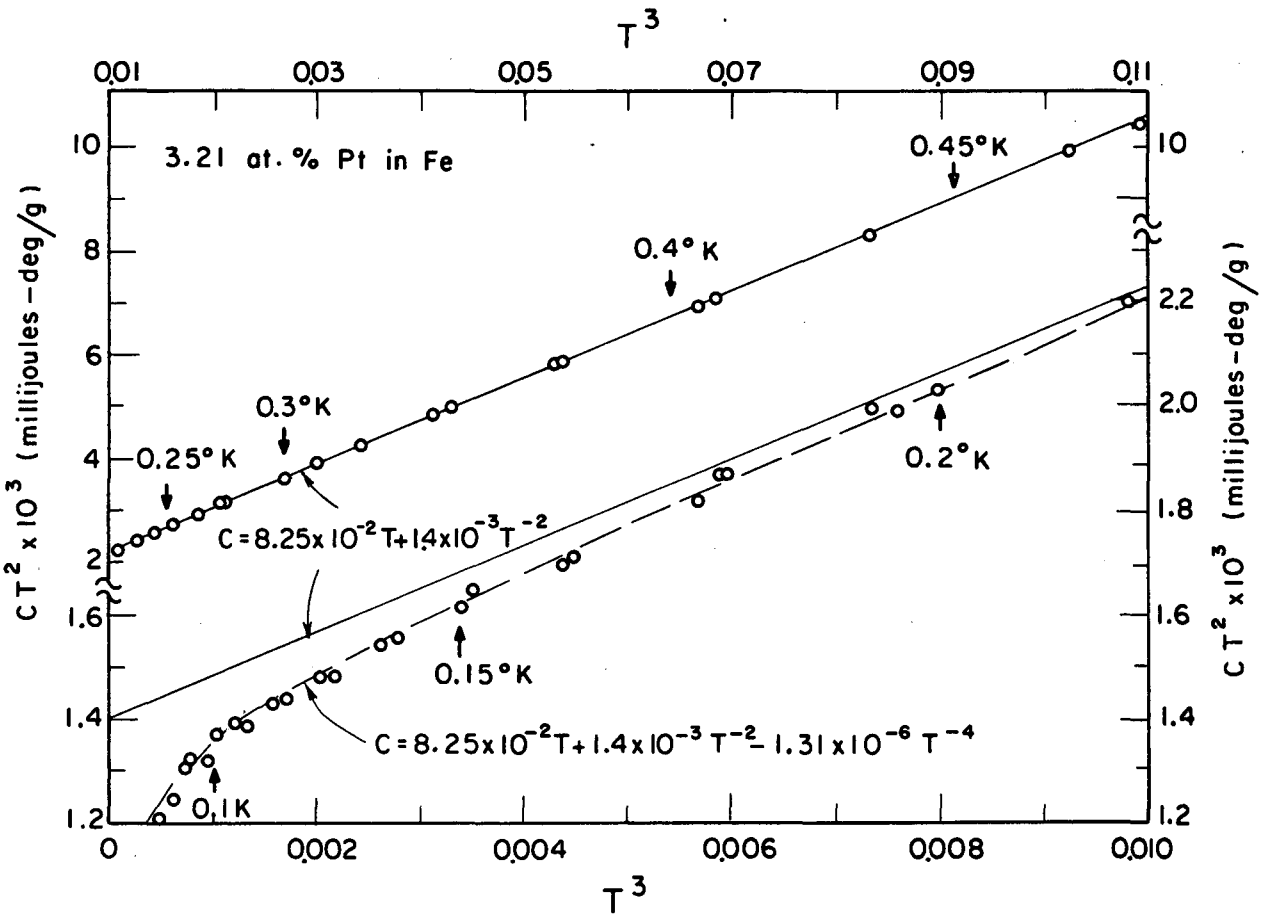
T 3
0.01
0.03
0.05
0.07
0.09
0.11
3.21 at. % Pt in Fe
0.45°K
0.4° K
0.3°K
0.25° K
0.2°K
0.15°K
0.1K
C = 8.25x10-2T+14x10-3T-2
C = 8.25x10-2T+1.4x10-3 T-2- 1.31x10-6 T-4
C T2 x 10 3 (millijoules - deg/g)
C T2 x10 3 (millijoules - deg /g)
0
0.002
0.004
0.006
0.008
0.010
T 3
MUB-4800

Fig. 9

and

$$C(\text{mJ g}^{-1}\ \text{deg}^{-1}) = 1.40\times10^{-3}T^{-2} - 1.31\times10^{-6}T^{-4} \qquad (16)$$

for the Os in Fe and Pt in Fe samples, respectively. As shown in Fig.9, the expected T^{-4} term is in good agreement with experiment for the Pt in Fe sample. For the Os in Fe sample, the expected T^{-4} term is about 2% of the total heat capacity at 0.1°K, which is only slightly more than the scatter in the data. It is difficult to put limits on the accuracy of the H_e values; we expect an error of no more than 2% in the total heat capacity near 0.1°K, which would introduce a comparable error in H_e, but errors associated with the presence of trace quantities of elements with large nuclear moments might add to the error. It seems unlikely that changes in H_e at iron nuclei brought about by the presence of the Os or Pt impurities would contribute significantly to the error.

In Table 6 the H_e values for Os and Pt are compared with those for neighbouring third-transition-group elements, all in dilute solution in Fe. For Os, Ir, Pt, and Au, the values are approximately the same, but for W and Re the values are smaller by approximately a factor of two.

The Mössbauer effect has been observed for the 99-keV (I = 3/2) state of Pt^{195} dissolved in Fe, but the expected six-line spectrum is incompletely resolved,[38,39] and no unambiguous assignment of H_e and the excited-state moment μ_{exc} has been made. Experiments on 10 at.% Pt in Fe give[40] 1200 kOe < H_e < 2900 kOe and -0.8nm < μ_{exc} < 0.17 nm. The value of H_e reported here therefore suggests the assignment μ_{exc} = -0.7nm.

Cameron et al.[41] have measured the temperature dependence of the γ-ray anisotropy from 4.7-sec Ir^{191m} formed in the decay of Os^{191}, which was dissolved in Fe. The interpretation of their experiment depends on

Table 6. Hyperfine fields at the nuclei of third-transition-group elements dissolved in iron. For W, Os, and Pt, the sign of H_e is not determined by the experiments. For Re and Ir, the sign of H_e has been determined in separate experiments[a] based on anistropy of γ rays from polarized nuclei.

Alloy	H_e at solute nucleus (kOe)	Method[b]	Reference
W-Fe	760	ME	c
Re-Fe	-610	C	d
	-670	C	e
Os-Fe	1400	C	This work
Ir-Fe	-1350	C	e
Pt-Fe	1390	C	This work
Au-Fe	-1420	ME	f

a. A.V. Kogan, V.D. Kul'kov, L.P. Nikitin, N.M. Reinov, M.F. Stel'mach, and M. Schott, Zh. Eksperim. i. Teor. Fix. 43, 828 (1962) (Translation: Soviet Phys.-JETP 16, 586 (1963)).

b. Method: ME = Mössbauer effect; C = heat capacity.

c. E. Kankeleit, Bull. Am. Phys. Soc. 10, 65 (1965).

d. O.V. Lounasmaa, C.H. Cheng, and P.A. Beck, Phys. Rev. 128, 2153 (1962).

e. A.V. Kogan, V.D. Kul'kov, L.P. Nikitin, N.M. Reihov, and M.F. Stel'makh, Zh. Eksperim. i. Teor. Fix. 45, 1 (1963) (Translation: Soviet Phys. -JETP 18, 1 (1964)).

f. R.W. Grant, M. Kaplan, D.A. Keller, and D.A. Shirley, Phys. Rev. 133, 1062 (1964).

whether the spin-lattice relaxation time of Ir in Fe is greated than or less than 4.7 sec. If it is much greater than 4.7 sec., the observed anisotropy is characteristic of the Os^{191}, and the assumption of the Schmidt single-particle value of the magnetic moment for the excited state leads to the assignment H_e = 5000 kOe. Cameron et al. concluded that this was unreasonably high, that the relaxation time must be smaller than 4.7 sec., and that the observed anisotropy was characteristic of Ir^{191m}. They then used the value of H_e for Ir in Fe quoted in Table 6 to calculate $|\mu|$ = 7.3±1.5nm for Ir^{191m}, which is in reasonable agreement with theoretical predictions. The value of H_e for Os in Fe reported here supports their analysis to the extent of showing that H_e for Os in Fe is in fact much less than 5000 kOe.

Table 7. Heat Capacity of Dilute Osmium in Iron

T (°K)	C mJ/gram-deg)	T (°K)	C (mJ/gram-deg)
0.08276	0.02345	0.4735	0.03998
0.08897	0.02171	0.5064	0.04287
0.1033	0.01880	0.5429	0.04580
0.1134	0.01818	0.5842	0.04950
0.1247	0.01746	0.6312	0.05326
0.1365	0.01742	0.6836	0.05755
0.1492	0.01763	0.7364	0.06201
0.1627	0.01804	0.7945	0.06700
0.1765	0.01860	0.8615	0.07272
0.1925	0.01899	0.9315	0.07801
0.2095	0.01996	0.9971	0.08461
0.2266	0.02112	1.088	0.09232
0.2448	0.02251	1.160	0.09676
0.2617	0.02344	0.4974	0.04199
0.2792	0.02479	0.5468	0.04610
0.2981	0.02622	0.5940	0.05026
0.3202	0.02790	0.6439	0.05427
0.3426	0.02971	0.6995	0.05898
0.3624	0.03185	0.7580	0.06379
0.3809	0.03258	0.8200	0.06851
0.4015	0103447	0.9019	0.07667
0.4218	0.03566	0.9868	0.08388
0.4447	0.03797	1.070	0.09001

Table 8. Heat Capacity of Dilute Platinum in Iron

T (°K)	C (mJ/gram-deg)	T (°K)	C (mJ/gram-deg)
0.07747	0.2011	0.2751	0.04119
0.08411	0.1768	0.2993	0.04028
0.09056	0.1597	0.3244	0.04026
0.09824	0.1370	0.3504	0.04034
0.09259	0.1539	0.3773	0.04096
0.1008	0.1352	0.4057	0.04191
0.1099	0.1149	0.4363	0.04326
0.1195	0.1007	0.4677	0.04490
0.1296	0.08821	0.5031	0.04716
0.1407	0.07880	0.5435	0.04968
0.1520	0.07135	0.5836	0.05246
0.1638	0.06322	0.6329	0.05581
0.1785	0.05721	0.7977	0.06800
0.1944	0.05291	0.2773	0.04106
0.1071	0.1212	0.3109	0.04014
0.1165	0.1055	0.3456	0.04017
0.1270	0.09162	0.3762	0.04090
0.1382	0.08117	0.4084	0.04210
0.1502	0.07159	0.4779	0.04551
0.1646	0.06323	0.5267	0.04828
0.1811	0.05691	0.5708	0.05142
0.1998	0.05085	0.6252	0.05550
0.2209	0.04658	0.6773	0.05944
0.2432	0.04335	0.7894	0.06800
0.2647	0.04174	0.8500	0.07228
0.1806	0.05718	0.9050	0.07762
0.1966	0.05141	0.9747	0.08266
0.2141	0.04807	1.155	0.09795
0.2331	0.04472	0.7234	0.06330
0.2528	0.04269	0.7914	0.06839
0.8636	0.07374	1.019	0.08676
0.9383	0.07992		

REFERENCES

1. For a full discussion and numerous references, see R. E. Watson and A. J. Freeman, Phys. Rev. 123, 2027 (1961).
2. E. Fermi, Z. Phys. 60, 320 (1930).
3. A. Abragam, J. Horowitz, and M. H. L. Pryce, Proc. Roy. Soc. (London) A230, 169 (1955).
4. R. M. Sternheimer, Phys. Rev. 86, 316 (1952).
5. W. Marshall, Phys. Rev. 110, 1280 (1958).
6. D. A. Goodlings and V. Heine, Phys. Rev. Letters 5, 370 (1960).
7. P. W. Anderson and A. M. Clogston, Bull. Am. Phys. Soc. 6, 124 (1961).
8. S. S. Hanna, J. Heberle, G. J. Perlow, R. S. Preston, and D. H. Vincent, Phys. Rev. Letters 4, 513 (1960).
9. V. Arp, D. Edmonds, and R. Petersen, Phys. Rev. Letters 3, 164 (1959).
10. A. C. Gossard and A. M. Portis, Phys. Rev. Letters 3, 164 (1959).
11. Y. Koi, A. Tsujimara, T. Hihara, and T. Kushida, J. Phys. Soc. Japan 17, Suppl. B1., 96 (1961).
12. R. L. Streever, Phys. Rev. Letters 10, 232 (1963).
13. J. S. Kasper and B. W. Roberts, Phys. Rev. 101, 537 (1956).
14. C. V. Heer and R. A. Ericson, Phys. Rev. 108, 896 (1957).
15. W. H. Lien (Ph.D.Thesis) University of California, Berkeley, (1962).
16. H. R. O'Neal (Ph.D.Thesis) University of California, Berkeley, (1963).
17. N. M. Senozan (Ph.D.Thesis) University of California, Berkeley (1965).
18. Y. L. Shen, (Department of Chemistry, University of California, Berkeley) Private communication.

REFERENCES (Continued)

19. N. E. Phillips, Phys. Rev. 134, A385 (1964).

20. Z. S. Basinski and J. W. Christian, J. Inst. Metals 80, 659 (1951).

21. R. S. Dean, J. R. Long, T. R. Graham, E. V. Potter, and E. T. Hayes, Trans. Am. Soc. Metals 34, 443 (1945).

22. G. E. Bacon, I. W. Duncan, J. H. Smith, and R. Street, Proc. Roy. Soc. (London) A241, 223 (1957).

23. D. Meneghetti and S. S. Sidhu, Phys. Rev. 105, 130 (1957).

24. D. Schlain and J. D. Prater, Trans. Electrochem. Soc. 94, 58 (1948).

25. S. Shinozaki, A. Arrott, H. Sato, and J. E. Zimmerman, Bull. Am. Phys. Soc. 8, 66 (1963).

26. D. Strominger, J. M. Hollander, and G. T. Seaborg, Rev. Mod. Phys. 30, 585 (1958).

27. L. W. McKeehan, Phys. Rev. 43, 913 (1933).

28. R. G. Scurlock and W. N. R. Stevens, Proc. VIII Int. Conf. Low Temp. Phys. London, 264 (1962).

29. P. N. Stetsenko and Yu. I. Avksent'ev, Zh. Eksperim. i. Teor. Fiz. 47, 806 (1964) (Translation: Soviet Phys.-JETP 20, 539 (1965)).

30. A. J. Bradley and J. Thewlis, Proc. Roy. Soc. (London) A115, 456 (1927).

31. J. Itoh, Y. Masuda, K. Asayama, and S. Kobayashi, J. Phys. Soc. Japan 18, 455 (1963); Y. Masuda, K. Asayama, S. Kobayashi, and J. Itoh, J. Phys. Soc. Japan, 19, 460 (1964).

32. L. M. Corliss, J. M. Hastings, and R. J. Weiss, Phys. Rev. Letters, 3, 211 (1959).

33. G. E. Bacon, Acta Cryst. 14, 823 (1961).

REFERENCES (Continued)

34. G. Shirane and W. J. Takei, J. Phys. Soc. Japan 17, Suppl. III, 35 (1962).

35. J. A. Payne and W. R. G. Kemp, Phil. Mag. 1, 918 (1956).

36. M. Weger, Phys. Rev. 128, 1505 (1962).

37. G. E. Bacon, Proc. Phys. Soc. 79, 938 (1962).

38. G. M. Rothberg, N. Benczer-Koller, and I. R. Harris, Rev. Mod. Phys. 36, 357 (1964).

39. A. B. Buyrn and L. Grodzins, Bull. Am. Phys. Soc. 9, 410 (1964).

40. N. Benczer-Koller, G. M. Rothberg, and J. R. Harris (Physics Department, Rutgers University), Private communication.

41. J. A. Cameron, I. A. Campbell, J. P. Compton, and R. A. G. Lines, Phys. Letters 10, 24 (1964).

FIGURE CAPTIONS

Part I

1. Schematic diagram of the apparatus.
2. Construction of a two-salt system.
3. The heat capacity of copper. ⊙: Sample A; o: Sample B.
4. The heat capacity of γ-manganese.
5. The heat capacity of chromium. ⊙: Sample A; o: Sample B.
6. The magnetic structures of γ-manganese and gold-manganese.
7. The heat capacity of gold-manganese.
8. The heat capacity of an alloy of 0.75 at.% Os in Fe.
9. The heat capacity of an alloy of 3.21 at.% Pt in Fe. The T^{-4} term of the dashed curve was calculated from the corresponding T^{-2} term determined in the straight-line region at higher temperatures.

II. HEAT CAPACITIES OF COPPER-MANGANESE ALLOYS BELOW 1°K

A. Introduction

Recently, considerable attention has been given to the anomalous behavior of different properties of dilute alloys of transition metals in non-magnetic hosts such as copper, silver, gold, zinc, etc.[1] There appear to be at least two types of these dilute alloys:[2] one typified by copper-manganese which shows both a resistance maximum and a minimum and a cooperative magnetic transition at low temperatures; and another typified by copper-iron which shows only a resistance minimum and also no evidence that the magnetic transition is cooperative in nature. So far most of the theoretical approaches to this problem are based on experimental results. Therefore, more well-designed experiments might be useful stimuli to the theoretical studies.

Among these dilute alloys, the copper-manganese system has been particularly thoroughly studied both experimentally and theoretically.[1] The equilibrium diagram[3] of the copper-manganese system shows a continuous solid solution at high temperatures between copper and the γ form of manganese. The face-centred cubic structure can be retained for quenched alloys except those with more than about 70 at.%Mn, which become face-centred tetragonal with an axial ratio increasing continuously with copper content.[4] The magnetic behavior of this system, on the other hand, is rather complicated. The manganese-rich alloys are typical antiferromagnetic due to the coupling between Mn ions as the manganese concentration becomes predominant.[5] No conclusive results but some indication of the presence of short-range magnetic ordering have been experimentally observed over a large range of intermediate alloy composi-

tions.[6] For manganese-rich alloys neutron diffraction experiments[5] give an effective magnetic moment which decreases with increasing copper content and extrapolates to $n_{eff} = 2.4\mu_B$ for γ-manganese. The apparent decrease with increasing copper content is perhaps a consequence of the concentration dependence of the Néel temperature. For dilute manganese alloys a number of magnetic measurements[7-11] suggest a limit of $n_{eff} = 4\mu_B$ at zero concentration and a slow decrease in n_{eff} with increasing manganese content.

The anomalous resistive bevahior of the dilute copper-manganese alloys--a maximum in addition to the minimum at a higher temperature --was first noted by Gerritsen and Linde.[12] Later investigations by Owen et al.[10,11] (electron spin resonance, nuclear magnetic resonance, and magnetic susceptibility measurements) and by Schmitt et al.[13] (magnetization, resistivity, and magnetoresistivity measurements) suggested a high-temperature paramagnetism with a positive Curie temperature but a gradual transition to antiferromagnetism with hystersis effects at low temperatures. This kind of behavior can be understood in terms of competing ferromagnetic and antiferromagnetic interactions of different strengths.[14]

The observation of an anomalous low-temperature heat capacity associated with the above effects was first carried out on a sample with 0.13 at.% Mn by de Nobel and du Chatenier.[15] Zimmerman and Hoare[16] made a further study above 2°K covering a wide concentration range. At the lowest temperatures of their measurements, the excess heat capacity (heat capacity of the alloy minus that of pure copper) seems to have a limit which is linear in temperature and independent of manganese concentration. To explain this anomaly, Overhauser[17,18] has postulated a

new mechanism for antiferromagnetism involving the concept of a static spin-density wave in the conduction band. Marshall[19] pointed out some objections to this mechanism and qualitatively explained the results by using the Ruderman-Kittel-Yosida spin interaction.[20,21] Both theories suggested that there is some degree of randomness in the alloy, which is essential to explain the anomalous heat capacity, but they gave different origins for this randomness. The Marshall theory has recently been made quantitative by Klein and Brout.[22]

Experimentally, however, the existence and behavior of the low-temperature limit of the anomalous heat capacity in dilute copper-manganese alloys was deduced from a narrow temperature range.[16] It is obvious that measurements at lower temperatures are desirable. So far such measurements have been reported by du Chatenier and de Nobel[23] for two alloys containing 1.0 and 0.13 at.% Mn, respectively. Their results gave no exact conclusion in this respect because of a steeply rising hyperfine heat capacity (which corresponds to a hyperfine field H_e = 470 kOe at Mn nuclei) at the low-temperature end of the measurements. Their results did show a smaller value of the excess heat capacity below 1°K than that extrapolated from the above 2°K measurements by Zimmerman and Hoare, but a good estimate is necessary to analyze for the contribution associated with the magnetic ordering, C_M. By examining their results, we found that their determination of this contribution was not satisfactory. At temperatures below 0.1°K, a large negative T^{-4} term in the heat capacity is expected from the reported H_e, but was not observed. Consequently, there is a discrepancy (10% at 0.1°K and 65% at 0.04°K, the lowest temperature of their measurements) between their reported H_e and their measured heat capacity which raises a question

about their measurements.

The copper-manganese system is not ideal for calorimetric investigation as far as the low-temperature behavior is concerned because of the presence of the hyperfine contribution. However, the other extensive investigations for this system enhance the interest in the calorimetric measurements and further measurements seem desirable. Furthermore, the hyperfine heat capacity itself is of some interest.

In Part II of this dissertation heat capacities of several dilute copper-manganese alloys below 1°K are reported and discussed. Measurements were also made for several high manganese content copper-manganese alloys for comparison with the previous work in the liquid helium temperatures by Zimmerman and Sato[24] and to obtain the hyperfine heat capacities.

B. Results and Discussion

1. Samples

The heat capacities of a total of eight copper-manganese alloy samples with 0.057, 0.14, 0.59, 1.07, 3.19, 43.5, 58.6, and 93.9 at.% Mn, respectively, have been measured below 1°K, with the same apparatus and procedures described in Part I. The first five dilute alloys, large cylindrical samples ranging from 80 to 400 g, were prepared by induction-melting high purity copper (American Smelting and Refining Company, 99.999% pure) and high manganese content copper-manganese alloy ingots in a graphite crucible under an argon atmosphere. Since carbon and manganese are rather reactive, the high manganese content alloy prepared previously in an arc furnace was used instead of pure manganese as the raw material to let manganese go into solution before coming into contact with the hot carbon wall. On the other hand, because of the high vapor pressure of manganese, the actual manganese concentrations of these dilute

alloy samples are different from the initial values of the raw materials before melting. Therefore, the values given above, which will be used as the basis for calculations in this work, are actually the average values of different colorimetric analysis results for thin disks cut from both ends of the cylindrical samples. In Table I all these values are listed. Table I shows a spread of about 10% in the values which presumably reflects the precision of the analysis and also the inhomogeneity of the samples.

The other three samples, about 10 g each, were supplied by the Scientific Laboratory, Ford Motor Company. The relatively small size gave a rapid quenching and perfect retention of γ-phase.

Table I. Manganese concentrations of dilute alloys used in this work. All values are in at.% Mn. c_i is the initial concentration of raw materials before melting; c_{top} and c_{bottom} are values determined colorimetrically for thin disks cut from the top and bottom ends of the cylindrical sample (Two sets of these values are obtained from independent analyses, except for the highest concentration one); and $c_{average}$ is the average of all analyses for the sample.

c_i	c_{top}	c_{bottom}	$c_{average}$
3.5	3.29	3.13	3.21
1.2	1.09	1.05	1.07
	1.13	1.03	
0.6	0.61	0.57	0.59
	0.59	0.57	
0.16	0.144	0.138	0.14
	0.145	0.134	
0.06	0.058	0.054	0.057
	0.059	0.056	

2. Data Analysis

Meausrements for the five dilute alloy samples were extended to about 0.06°K, where the T^{-4} term in the hyperfine heat capacity C_N should become observable and could be used as a check for the assignment of the H_e value. Since the magnetic heat capacity C_M associated with the Mn spin ordering is large as expected but not so simple as linear in temperature, the analysis of experimental data is carried out by determining the hyperfine heat capacity first. This was done for each sample as follows. By plotting CT^2 versus T^3 for a certain temperature range at which both the T^{-4} term and C_M are relatively small compared with the T^{-2} term in the heat capacity (therefore the deviation from the linear temperature dependence of C_M is also insignificant) and extrapolating to T = 0, the T^{-2} term was determined. Since it is impossible by these measurements alone to determine the contributions from Mn and Cu nuclei separately, the value of H_e at Mn nuclei is calculated from this observed T^{-2} term by neglecting completely the Cu nuclei contribution. Therefore, this value should be considered only the upper limit of H_e at Mn nuclei. The expected T^{-4} term is then calculated from the H_e value, and compared with the lower temperatures points. Figs. 1 and 2 show these plots for the five dilute alloys and also show that the calculated T^{-4} term is at least consistent with this analysis of the data. The values of C_N and H_e thus obtained are listed in Table 2. The scatter of the H_e values (around an average of 305 kOe) is believed to arise from the uncertainties of the average manganese concentrations $c_{average}$ discussed previously. Since C_N is proportional to cH_e^2, an uncertainty of 10% in c will introduce a corresponding uncertainty of 5% in H_e.) These results are substantially different from

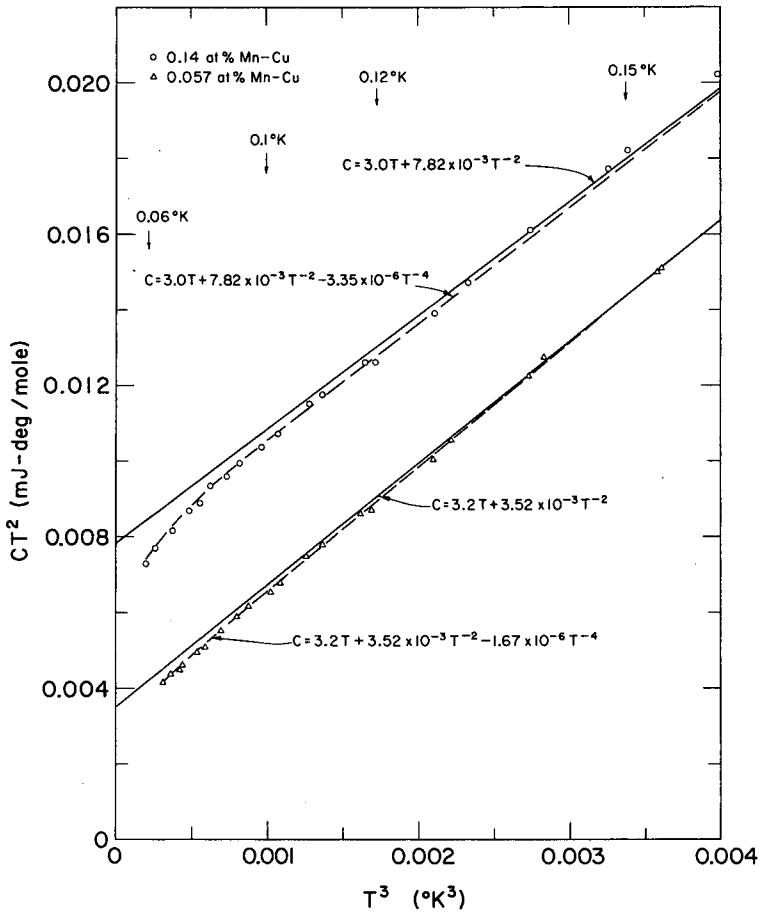
o 0.14 at % Mn-Cu
Δ 0.057 at % Mn-Cu
0.12°K
0.15°K
0.1°K
C=3.0T+7.82x10⁻³T⁻²
0.06°K
C=3.0T+7.82x10⁻³T⁻²-3.35x10⁻⁶T⁻⁴
C=3.2T+3.52x10⁻³T⁻²
C=3.2T+3.52x10⁻³T⁻²-1.67x10⁻⁶T⁻⁴
CT² (mJ-deg/mole)
0.020
0.016
0.012
0.008
0.004
0
0.001
0.002
0.003
0.004
T³ (°K³)

Fig. 1

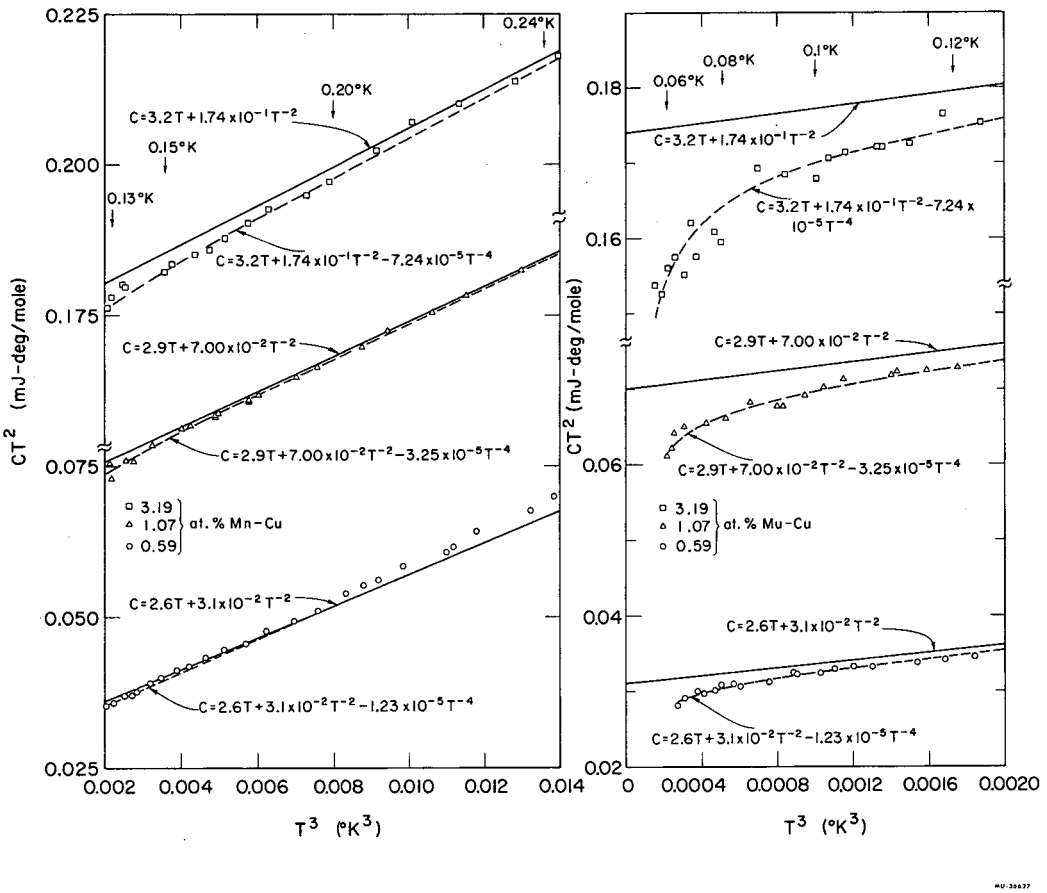
0.225
0.200
0.175
0.075
0.050
0.025
0.24°K
0.20°K
0.15°K
0.13°K
C=3.2T+1.74x10⁻¹T⁻²
C=3.2T+1.74x10⁻¹T⁻²-7.24x10⁻⁵T⁻⁴
C=2.9T+7.00x10⁻²T⁻²
C=2.9T+7.00x10⁻²T⁻²-3.25x10⁻⁵T⁻⁴
□ 3.19
△ 1.07
○ 0.59
at. % Mn-Cu
C=2.6T+3.1x10⁻²T⁻²
C=2.6T+3.1x10⁻²T⁻²-1.23x10⁻⁵T⁻⁴
CT² (mJ-deg/mole)
0.002 0.004 0.006 0.008 0.010 0.012 0.014
T³ (°K³)
0.18
0.16
0.06
0.04
0.02
0.06°K
0.08°K
0.1°K
0.12°K
C=3.2T+1.74x10⁻¹T⁻²
C=3.2T+1.74x10⁻¹T⁻²-7.24x10⁻⁵T⁻⁴
C=2.9T+7.00x10⁻²T⁻²
C=2.9T+7.00x10⁻²T⁻²-3.25x10⁻⁵T⁻⁴
□ 3.19
△ 1.07
○ 0.59
at. % Mu-Cu
C=2.6T+3.1x10⁻²T⁻²
C=2.6T+3.1x10⁻²T⁻²-1.23x10⁻⁵T⁻⁴
CT² (mJ-deg/mole)
0 0.0004 0.0008 0.0012 0.0016 0.0020
T³ (°K³)

Fig. 2

Table 2. Hyperfine heat capacities C_N and hyperfine fields H_e at Mn nuclei of γ-manganese and copper-manganese alloys. The H_e values are determined from the observed T^{-2} terms in C_N by neglecting the contributions from Cu nuclei. For the dilute alloys, the T^{-4} terms are calculated from the corresponding H_e values (see text). The sign of H_e is not determined by the experiments.

Alloy (at.% Mn)	Temperature range of measurements (°K)	C_N (mJ/mole-deg)	H_e (kOe)
0.057	0.067-1.2	$0.00352T^{-2}$ $-1.67\times10^{-6}T^{-4}$	315
0.14	0.058-1.1	$0.00782T^{-2}$ $-3.35\times10^{-6}T^{-4}$	300
0.59	0.065-1.2	$0.0310T^{-2}$ $-1.23\times10^{-5}T^{-4}$	290
1.07	0.060-1.2	$0.0700T^{-2}$ $-3.25\times10^{-5}T^{-4}$	324
3.19	0.054-1.0	$0.174T^{-2}$ $-7.24\times10^{-5}T^{-4}$	298
43.5	0.18-1.1	$1.00T^{-2}$	192
58.6	0.17-1.2	$0.930T^{-2}$	160
93.9	0.17-1.0	$0.360T^{-2}$	79
100 (γ-Mn)	0.066-4.2	$0.264T^{-2}$	65

those of du Chatenier and de Nobel[23] (H_e = 470 kOe for 1.0 and 0.13 at.% Mn samples on the basis of the same assumption). At $T \leq 0.1$°K our measured heat capacities and theirs are both closely proportional to manganese content but our value of the proportionality constant is less than half of theirs. However, as pointed out in the Introduction, the temperature dependence of their heat capacity is inconsistent with their own assignment H_e = 470 kOe.

The sum of the electronic and magnetic heat capacities is finally determined by subtracting the hyperfine contribution from the measured heat capacity, and is shown in a plot of $(C-C_N)/T$ versus T in Fig. 3. Since the hyperfine contribution predominates in the low-temperature end, Fig. 3 shows only points above a temperature for which $(C-C_N)$ is still about 20% of the total heat capacity. (This temperature is different for different alloys.) It should be noted that the points at these temperatures, therefore, have possible errors up to 5% as the total heat capacity has an estimated accuracy of about 1%. Furthermore, there is a possible uncertainty associated with the difficulty in assigning the correct T^{-2} term. This factor might be related to the apparent leveling off of the $(C-C_N)/T$ values with temperature at the low-temperature end for several alloys, which, therefore, should not be taken into consideration too seriously.

For the alloys with 43.5, 58.6, and 93.9 at.% Mn, the total heat capacity can be well separated into the T and T^{-2} terms by plotting CT^2 versus T^3 as shown in Fig. 4, in which the results for γ-manganese are also included for comparison. The straight lines give

$$C(\text{mJ mole}^{-1}\ \text{deg}^{-1}) = 4.07T + 1.00T^{-2} \qquad (1)$$

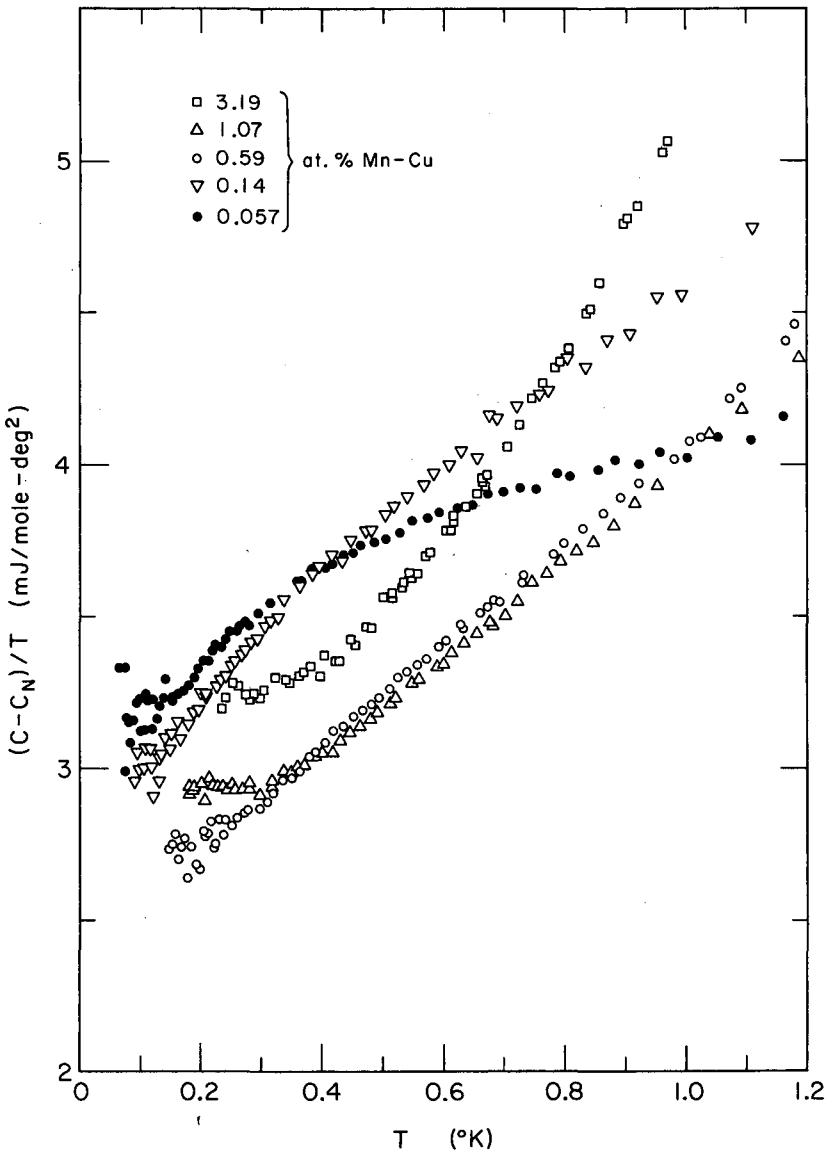
3.19
1.07
0.59
0.14
0.057
at. % Mn-Cu
5
4
3
2
0
0.2
0.4
0.6
0.8
1.0
1.2
T (°K)
(C-C_N)/T (mJ/mole-deg²)
MU-36624

Fig. 3

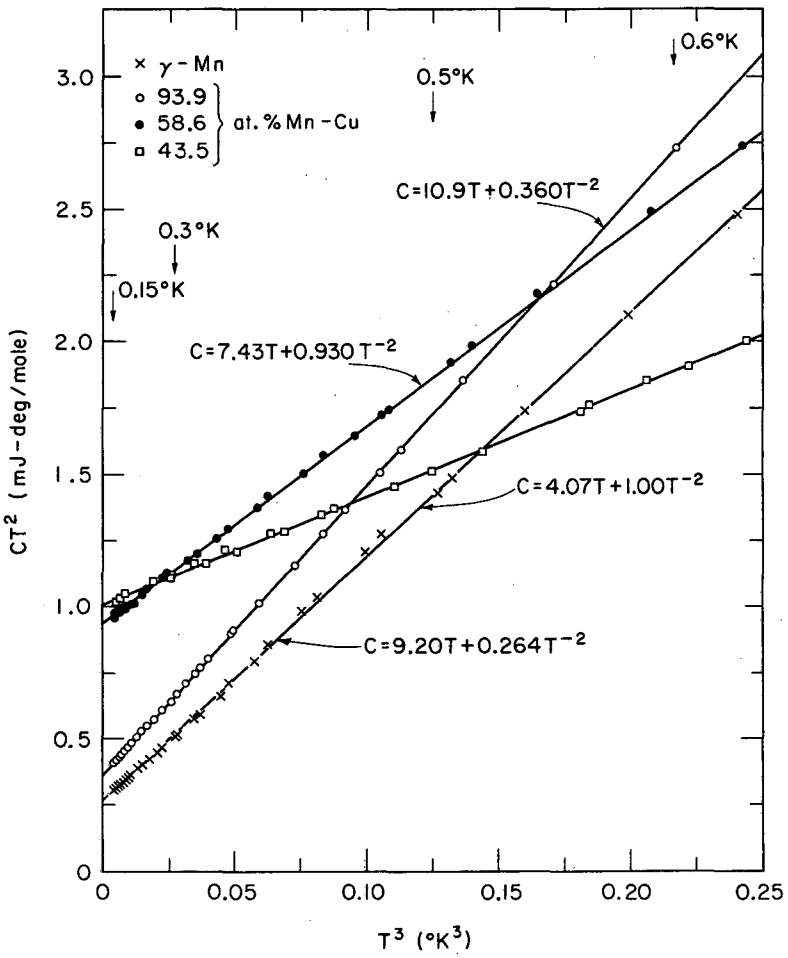
× γ-Mn
○ 93.9
● 58.6
□ 43.5
at. % Mn-Cu
0.6°K
0.5°K
0.3°K
0.15°K
C=10.9T+0.360T⁻²
C=7.43T+0.930T⁻²
C=4.07T+1.00T⁻²
C=9.20T+0.264T⁻²
CT² (mJ-deg/mole)
T³ (°K³)
0
0.5
1.0
1.5
2.0
2.5
3.0
0.05
0.10
0.15
0.20
0.25
MU-36625

Fig. 4

for the 45.5 at.% Mn-Cu sample,

$$C(\text{mJ mole}^{-1}\ \text{deg}^{-1}) = 7.43T + 0.930T^{-2} \qquad (2)$$

for the 58.6 at.% Mn-Cu sample, and

$$C(\text{mJ mole}^{-1}\ \text{deg}^{-1}) = 10.9T + 0.360T^{-2} \qquad (3)$$

for the 93.9 at.% Mn-Cu sample. Again we assume that the contribution to C_N from Cu nuclei is negligible, and calculate the H_e value for Mn nuclei from the observed T^{-2} term. The C_N and H_e values for these three samples and for γ-manganese are also listed in Table 2. For these alloys the linear term is somewhat higher than that determined by Zimmerman and Sato[24] in the liquid-helium temperatures, but the discrepancy is not serious.

3. Discussion

a. Hyperfine Heat Capacity

In Fig. 5 a plot of H_e versus the manganese content for the eight alloys and γ-manganese shows a striking feature -- a more or less linear relation between these two factors. However, one should keep in mind that for all alloys the H_e values obtained in this work are only upper limits for the H_e values at Mn nuclei. There is no way at the present time to justify in general the assumption that the contribution to C_N from Cu nuclei is negligible. However, Cameron et al.,[25] using the nuclear polarization method, have determined the H_e value at Mn nuclei in a very dilute manganese in copper sample to be 280 kOe. This is in good agreement with our results for the dilute alloys in view of the experimental uncertainties in both methods. On the other hand, if 280 kOe is taken as the correct value for H_e at Mn nuclei for the dilute

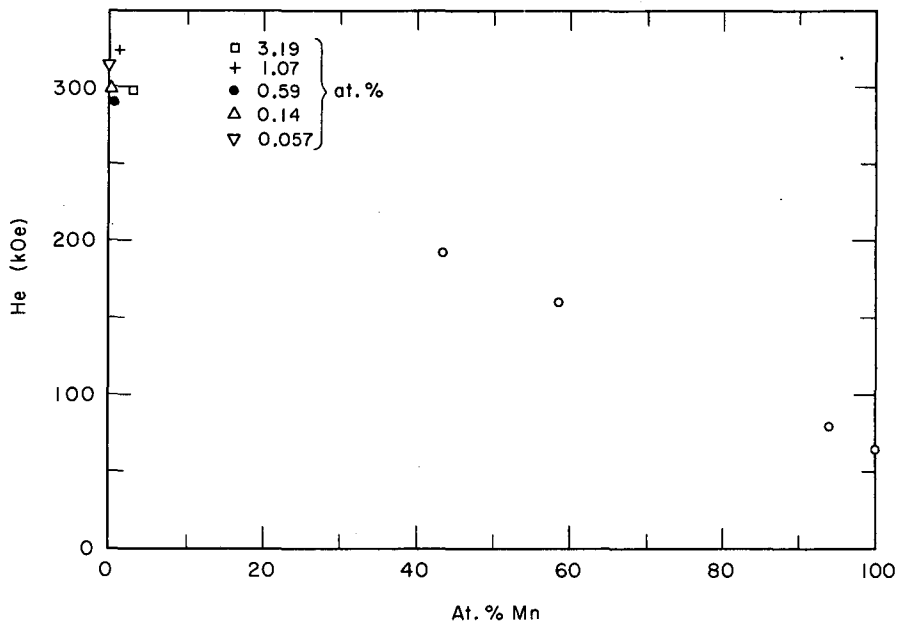
3.19
1.07
0.59
0.14
0.057
at. %
300
200
100
0
He (kOe)
0
20
40
60
80
100
At. % Mn
MU-36623

Fig. 5

alloys and the extra hyperfine contribution to the heat capacity is assumed to come from the 12 nearest Cu ion neighbours of each Mn ion, the root-mean-square hyperfine field at these Cu nuclei is 45 kOe.

The only definite conclusion that one can state is that H_e increases more rapidly than n_{eff} in going from γ-manganese to the dilute alloys, in contrast with the often-applied rule that H_e/n_{eff} is a constant for an ion in a given system. Furthermore, the H_e/n_{eff} ratios are appreciably less, even for the dilute alloys, than that suggested by the core-polarization calculations.[26] In this respect the results are similar to those for the other antiferromagnets studied in Part I.

For intermediate concentrations it is not clear how to interpret the apparent H_e values. The small increase of H_e from γ-manganese to the 93.9 at.% Mn-Cu alloy (both have nearly the same face-centred tetragonal and antiferromagnetic structures and also moments of the manganese ions) might be of the same origin as that suggested in Part I for the interpretation of the results for gold-manganese. That is, for each Mn ion, the number of nearest anti-parallel Mn ion neighbours is less in the alloy than it is in the pure metal. It is also possible that the Cu nuclei contribute to the measured C_N since, unlike Au nuclei, they have appreciable moment.

b. Electronic and Magnetic Heat Capacities

For the dilute alloys, the electronic heat capacity is presumably close to the pure copper value, because it seems unlikely that a large change in the density of states at the Fermi surface is produced by introducing a small amount of impurity. This expectation is supported by heat capacity measurements on a number of dilute solutions of non-

magnetic impurities in copper. For example, from their very recent work on a series of face-centred-cubic copper-zinc alloys with zinc content from 0 to 38.4 at.%, Isaacs et al.[27] found that the change in the electronic heat capacity is less than a few percent. $(C-C_N)$ for the dilute copper-manganese alloys as shown in Fig. 3, therefore, must include the magnetic contribution C_M and a linear electronic contribution close to that of pure copper, 0.70T mJ/mole-deg.

C_M for all the dilute alloys at low temperatures shows a similar temperature dependence and only a weak dependence on concentration. The overlapping of the points for different alloys in Fig. 3 might be explained by the fact that the Mn spin ordering temperatures are proportional to the manganese contents. For the two alloys with 0.057 and 0.14 at.% Mn the observed C_M values are still near the maxima of the anomalies, whereas for the other three samples they are already in the low-temperature tail regions. For the 0.057 at.% Mn sample it is clear that there is a broad maximum in C_M near 1°K. For a 0.05 at.% Mn in Cu sample, Schmitt et al.[13] also found a resistivity maximum at about 1°K. The resistivity maxima moved to higher temperatures for higher manganese concentrations.[13]

For the 0.057 at.% Mn sample, the excess entropy associated with the anomaly below 1.2°K can be calculated by extrapolating the $(C-C_N)/T$ to T = 0°K. The result is insensitive to the details of the extrapolation from 0.06°K, and is about 3.6 mJ/mole-deg. This value is about one half of the total entropy expected for the ordering of Mn ions with a spin of 2, suggested by magnetic measurements.[7-11] The shape of the anomaly suggests that the total entropy may be consistent with this spin assignment. For the more concentrated alloys, for which there are

measurements above 1°K,[15,16] the uncertainty in the assignment of lattice and electronic entropies prevents a determination of the magnetic entropy.

The low-temperature limit of C_M suggested by Zimmerman and Hoare[16] from their above 2°K measurements -- linear in temperature and independent of manganese concentration -- is not observed, although the highest temperatures points in our measurements are in good agreement with their extrapolations. Below 1°K, the $(C-C_N)/T$ value keeps decreasing with temperature instead of approaching a constant value. Although C_M may become proportional to T in the limit $T \to 0$, another term, approximately proportional to T^2, is still important in the temperature range of our measurements.

So far theoretical work on C_M[17-19] has given a qualitative low-temperature limit of the same kind suggested by Zimmerman and Hoare.[16] Recently Klein and Brout[22] made a quantitative calculation and gave a $\lim_{T \to 0} (C/T)$ value of 4.3 mJ/mole-deg^2, which seemed to be in agreement with the extrapolation of the above 2°K measurements by Zimmerman and Hoare. Our results show that, if there is such a limit, it is smaller than that predicted by Klein and Brout. They do not clearly establish either the presence or the absence of a non-zero limiting value of C_M/T. The experimental points at the lowest temperatures are remarkably insensitive to the manganese concentration: at 0.2°K all samples with 0.057 to 3.21 at.% Mn fall within 30% of each other in C_M/T, and, to this extent, agree with the theory. Experimentally it seems unlikely that any more definite conclusion for this system can be made. The presence of the hyperfine heat capacity is the great problem.

Table 3. Heat Capacities of Copper-Manganese Alloys

T (°K)	C (mJ/mole-deg)	T (°K)	C (mJ/mole-deg)
a. 93.9 at.% Mn-Cu:		0.6505	7.903
0.1766	13.33	0.7040	8.292
0.1953	11.62	0.7641	8.856
0.2150	10.17	0.8253	9.457
0.2346	9.107	0.8954	10.16
0.2553	8.386	0.9635	10.92
0.2815	7.643	0.9891	10.99
0.3035	7.237		
0.1667	14.75	b. 5816 at.% Mn-Cu:	
0.1835	12.61	0.1691	34.03
0.2034	10.89	0.1855	28.35
0.2244	9.617	0.2014	24.64
0.2457	8.709	0.2229	20.23
0.2678	7.972	0.2489	16.99
0.2942	7.412	0.2819	13.93
0.3275	6.962	0.3175	11.64
0.3330	6.930	0.3508	10.22
0.3656	6.706	0.3886	9.110
0.4374	6.654	0.4242	8.360
0.4718	6.771	0.4568	7.891
0.5151	6.979	0.4769	7.673
0.3152	7.121	0.5190	7.355
0.3413	6.850	0.6238	7.041
0.3669	6.715	0.7023	6.939
0.3895	6.628	0.7657	7.116
0.4177	6.612	0.8268	7.522
0.4512	6.701	0.8882	7.829
0.4833	6.818	0.9562	8.265
0.5545	7.195	1.015	8.627
0.6010	7.552	1.103	9.020

Table 3. (Continued)

T (°K)	C (mJ/mole-deg)	T (°K)	C (mJ/mole-deg)
0.1715	32.50	0.5653	5.421
0.1891	27.24	0.6247	5.129
0.2052	23.52	0.6662	4.986
0.2276	20.09	0.7698	4.870
0.2550	16.46	0.8029	4.797
0.2892	13.43	0.8946	4.895
0.3294	11.03	0.9578	5.001
0.3619	9.903	1.002	5.163
0.3966	9.013	1.039	5.206
0.4378	8.240	1.051	5.310
0.4738	7.682	1.129	5.495
0.5081	7.447	0.2954	12.76
0.5479	7.288	0.3380	10.20
0.5919	7.110	0.3706	8.770
0.7307	7.175	0.4091	7.674
0.8941	7.906	0.4443	6.952
1.053	8.838	0.4797	6.301
1.162	9.105	0.5237	5.759
		0.5687	5.433
c. 43.5 at.% Mn-Cu:		0.5900	5.314
0.1750	33.25	0.6051	5.194
0.1902	28.57	0.6347	5.026
0.2061	24.67	0.6778	4.977
0.2669	15.33	0.6916	4.884
0.2958	12.76	0.7484	4.798
0.3249	10.98	0.8003	4.857
0.3581	9.448	0.8301	4.858
0.3986	8.015	0.8711	4.816
0.4359	7.087	0.8772	4.885
0.4994	6.063	0.9360	4.998

Table 3. (Continued)

T (°K)	C (mJ/mole-deg)	T (°K)	C (mJ/mole-deg)
0.9851	4.983	0.1635	6.920
0.9938	5.056	0.1728	6.288
1.067	5.346	0.1847	5.644
		0.1991	4.977
d. 3.19 at.% Mn-Cu:		0.2162	4.427
0.05350	53.71	0.2343	3.892
0.05714	46.76	0.2527	3.537
0.06033	42.85	0.1681	6.573
0.06379	38.69	0.1793	5.919
0.06745	34.12	0.1939	5.181
0.07199	30.41	0.2092	4.612
0.07758	26.72	0.2248	4.158
0.09431	18.94	0.2414	3.744
0.09994	16.81	0.2600	3.407
0.1051	15.52	0.2738	3.196
0.1099	14.25	0.2886	3.014
0.1145	13.15	0.3042	2.859
0.06988	33.20	0.3233	2.723
0.07934	25.33	0.3450	2.588
0.08855	21.59	0.3698	2.491
0.1020	16.37	0.3962	2.413
0.1107	14.05	0.4215	2.389
0.1187	12.53	0.4477	2.400
0.1276	10.83	0.4738	2.415
0.1366	9.632	0.4998	2.474
0.1558	7.560	0.5288	2.526
0.1234	11.53	0.5570	2.588
0.1296	10.58	0.2797	3.113
0.1361	9.703	0.2979	2.914
0.1530	7.787	0.3409	2.612

Table 3. (Continued)

T (°K)	C (mJ/mole-deg)	T (°K)	C (mJ/mole-deg)
0.3623	2.518	0.6080	2.770
0.3822	2.462	0.6526	2.956
0.4044	2.423	0.6697	3.040
0.4283	2.382	0.7249	3.328
0.4520	2.389	0.7825	3.662
0.4812	2.415	0.8380	4.020
0.5132	2.495	0.8991	4.529
0.5430	2.567	0.9600	5.019
0.5768	2.663		
0.6162	2.820	e. 1.07 at.% Mn-Cu:	
0.6636	3.009	0.06010	16.92
0.7645	3.560	0.06327	16.05
0.8048	3.797	0.06211	16.13
0.8560	4.179	0.06742	14.30
0.9193	4.663	0.07492	11.65
0.6052	2.762	0.08075	10.14
0.6365	2.889	0.08685	9.042
0.6692	3.033	0.09397	7.669
0.7050	3.214	0.1014	6.836
0.7447	3.458	0.1091	0.035
0.7909	3.713	0.1167	5.327
0.8423	4.043	0.09273	7.874
0.9013	4.550	0.09792	7.217
0.9679	5.089	0.1048	6.481
0.5130	2.486	0.1127	5.691
0.5448	2.561	0.1207	5.004
0.6154	2.801	0.1296	4.345
0.6646	3.006	0.1401	3.862
0.5330	2.534	0.1620	3.113
0.5693	2.641	0.1706	2.878

Table 3. (Continued)

T (°K)	C (mJ/mole-deg)	T (°K)	C (mJ/mole-deg)
0.1794	2.669	0.5225	1.943
0.1287	4.564	0.5587	2.062
0.1371	4.039	0.5999	2.200
0.1483	3.577	0.6818	2.518
0.1590	3.210	0.3174	1.623
0.1700	2.890	0.3366	1.620
0.1822	2.613	0.3589	1.618
0.1965	2.369	0.3858	1.642
0.2114	2.177	0.4159	1.675
0.2260	2.020	0.4472	1.743
0.2420	1.895	0.4783	1.818
0.2599	1.790	0.5118	1.912
0.2792	1.715	0.5490	2.031
0.1697	2.896	0.5919	2.179
0.1793	2.668	0.6340	2.334
0.1915	2.447	0.6764	2.505
0.2063	2.223	0.7218	2.695
0.2199	2.080	0.7682	2.917
0.2350	1.946	0.8201	3.142
0.2518	1.835	0.8811	3.441
0.2699	1.745	0.9518	3.820
0.2792	1.712	1.039	4.329
0.2958	1.657	0.6122	2.253
0.3162	1.630	0.6542	2.415
0.3411	1.615	0.6998	2.594
0.3701	1.625	0.7438	2.811
0.3994	1.656	0.7929	3.029
0.4285	1.706	0.8461	3.266
0.4615	1.778	0.9146	3.624
0.4905	1.850	0.9954	4.062

Table B. (continued)

T (°K)	C (mJ/mole-deg)	T (°K)	C (mJ/mole-deg)
1.091	4.623	0.1839	1.409
1.186	5.211	0.1965	1.320
		0.2095	1.280
f. 0.59 at.% Mn-Cu:		0.2223	1.231
0.06471	6.716	0.2365	1.208
0.06925	6.076	0.1470	1.809
0.07437	5.380	0.1570	1.673
0.07949	4.876	0.1668	1.555
0.08454	4.285	0.1784	1.433
0.07224	5.755	0.1910	1.352
0.07738	5.029	0.2027	1.313
0.08279	4.512	0.2142	1.274
0.09104	3.767	0.2276	1.238
0.09658	3.450	0.2065	1.294
0.1032	3.088	0.2236	1.231
0.1093	2.780	0.2401	1.214
0.1155	2.524	0.2579	1.193
0.1225	2.289	0.2761	1.194
0.1306	2.103	0.2960	1.203
0.1394	1.909	0.3201	1.236
0.09591	3.510	0.3491	1.290
0.1009	3.186	0.3779	1.367
0.1063	2.940	0.4044	1.436
0.1190	2.407	0.4351	1.531
0.1265	2.213	0.4665	1.629
0.1361	1.998	0.4951	1.727
0.1415	1.882	0.5243	1.840
0.1514	1.744	0.5567	1.962
0.1615	1.607	0.5925	2.105
0.1723	1.507	0.6317	2.263

Table 5. (Continued)

T (°K)	C (mJ/mole-deg)	T (°K)	C (mJ/mole-deg)
0.6706	2.433	1.025	4.224
0.2504	1.195	1.089	4.655
0.2730	1.192	1.178	5.282
0.3093	1.219		
0.3344	1.266	g. 0.14 at.% Mn-Cu:	
0.3622	1.319	0.05792	2.176
0.2886	1.392	0.06378	1.893
0.4176	1.479	0.07214	1.567
0.4500	1.578	0.07850	1.411
0.4824	1.680	0.09537	1.286
0.5110	1.784	0.09346	1.138
0.5394	1.897	0.1023	1.024
0.5730	2.019	0.1111	0.9531
0.6030	2.147	0.1198	0.8778
0.6287	2.259	0.1325	0.8381
0.6585	2.382	0.1482	0.8037
0.6906	2.517	0.08218	1.318
0.7296	2.691	0.09016	1.179
0.7763	2.921	0.09872	1.064
0.8282	3.181	0.1086	0.9733
0.8925	3.515	0.1181	0.8998
1.006	4.136	0.1282	0.8426
1.072	4.549	0.1399	0.8249
1.164	5.156	0.1502	0.8081
0.6825	2.487	0.1585	0.8052
0.7312	2.727	0.1854	0.8141
0.7979	3.030	0.1961	0.8374
0.8626	3.350	0.2083	0.8527
0.9196	3.662	0.2226	0.8839
0.9800	3.974	0.2381	0.9228

Table 5. (Continued)

T (°K)	C (mJ/mole-deg)	T (°K)	C (mJ/mole-deg)
0.2545	0.9718	0.4297	1.622
0.2718	1.025	0.4686	1.805
0.2915	1.088	0.5039	1.959
0.3128	1.169	0.5399	2.128
0.3345	1.255	0.5824	2.338
0.3657	1.377	0.6287	2.561
0.3945	1.495	0.6725	2.814
0.1651	0.7972	0.7191	3.026
0.1791	0.8071	0.7724	3.287
0.1942	0.8270	0.8333	3.609
0.2124	0.8602	0.9055	4.019
0.2316	0.9069	0.9928	4.535
0.2490	0.9559	1.107	5.289
0.2671	1.010		
0.2842	1.065		
0.3033	1.134	h. 0.057 at.% Mn-Cu:	
0.3258	1.212	0.06727	0.9202
0.3808	1.401	0.07479	0.7997
0.4125	1.572	0.08373	0.7258
0.4452	1.710	0.09286	0.6835
0.4802	1.851	0.1008	0.6443
0.5175	2.025	0.07092	0.8697
0.5670	2.255	0.07591	0.8004
0.6075	2.457	0.08113	0.7517
0.6549	2.652	0.08857	0.7009
0.6864	2.867	0.09571	0.6727
0.7575	3.220	0.1029	0.6391
0.8027	3.500	0.1111	0.6314
0.8704	3.847	0.1192	0.6114
0.9522	4.339	0.1305	0.6188

Table 3. (Continued)

T (°K)	C (mJ/mole-deg)	T (°K)	C (mJ/mole-deg)
0.1415	0.6369	0.4158	1.546
0.1080	0.6398	0.4497	1.686
0.1175	0.6242	0.4831	1.831
0.1280	0.6129	0.5274	2.001
0.1397	0.6274	0.5743	2.207
0.1534	0.6419	0.6223	2.407
0.1701	0.6732	0.6719	2.633
0.1879	0.7173	0.7252	2.852
0.2044	0.7677	0.7885	3.134
0.2172	0.8091	0.8550	3.408
0.2317	0.8535	0.9215	3.687
0.2471	0.9063	1.004	4.043
0.2623	0.9595	1.106	4.514
0.2802	1.016	0.3632	1.338
0.3020	1.093	0.4030	1.497
0.1529	0.6401	0.4342	1.625
0.1641	0.6599	0.4641	1.748
0.1787	0.6938	0.5035	1.904
0.1954	0.7394	0.5471	2.094
0.2101	0.7820	0.5932	2.288
0.2238	0.8294	0.6453	2.507
0.2398	0.8807	0.6993	2.739
0.2562	0.9371	0.7507	2.950
0.2719	0.9927	0.8102	3.216
0.2908	1.061	0.8812	3.545
0.3127	1.143	0.9558	3.861
0.3566	1.314	1.052	4.308
0.3823	1.419	1.158	4.817

REFERENCES

1. For a recent coverage see G. J. van den Berg, Prog. Low Temp. Phys. Vol. IV, 194 (North Holland Publishing Co., Amsterdam, 1964).
2. D. L. Martin, Proc. VIII Int. Conf. Low Temp. Phys. 243 (1962).
3. R. S. Dean, J. R. Long, T. R. Graham, E. V. Potter, and E. T. Hayes, Trans. Am. Soc. Metals 34, 443 (1945).
4. Z. S. Basinski and J. W. Christian, J. Inst. Metals 80, 659 (1952).
5. G. E. Bacon, I. W. Dunmur, J. H. Smith, and R. Street, Proc. Roy. Soc. (London) A241, 223 (1957).
6. D. Meneghetti and S. S. Sidhu, Phys. Rev. 105, 130 (1956).
7. S. Valentiner and G. Becker, Z. Phys. 80, 735 (1933).
8. G. Gustafsson, Ann. Phys. Lpz. 25, 545 (1936).
9. H. P. Myers, Canad. J. Phys. 34, 527 (1956).
10. J. Owen, M. E. Browne, W. D. Knight, and C. Kittel, Phys. Rev. 102, 1501 (1956).
11. J. Owen, M. E. Browne, V. Arp, and A. F. Kip, J. Phys. Chem. Solids 2, 85 (1957).
12. A. N. Gerritsen and J. O. Linde, Physica 17, 573, 584 (1951); 18, 877 (1952).
13. R. W. Schmitt and I. S. Jacobs, J. Phys. Chem. Solids 3, 324 (1957).
14. J. S. Kouvel, J. Phys. Chem. Solids 21, 57 (1961).
15. J. de Nobel and F. J. du Chatenier, Physica 25, 969 (1959).
16. J. E. Zimmerman and F. E. Hoare, J. Phys. Chem. Solids 17, 52 (1960).
17. A. W. Overhauser, Phys. Rev. Letters 3, 414 (1959).
18. A. W. Overhauser, J. Phys. Chem. Solids 13, 71 (1959).
19. W. Marshall, Phys. Rev. 118, 1519 (1960).

20. M. A. Ruderman and C. Kittel, Phys. Rev. 96, 99 (1954).

21. K. Yoshida, Phys. Rev. 106, 893 (1957).

22. M. W. Klein and R. Brout, Phys. Rev. 132, 2412 (1963).

23. F. J. de Chatenier and J. de Nobel, Physica 28, 181 (1962).

24. J. E. Zimmerman and H. Sato, J. Phys. Chem. Solids 21, 71 (1961).

25. J. A. Cameron, I. A. Campbell, J. P. Compton, M. F. Grant, R. W. Hill and R. A. G. Lines, IX Int. Conf. Low Temp. Phys. (1964).

26. R. E. Watson and A. J. Freeman, Phys. Rev. 123, 2027 (1961).

27. L. L. Isaacs and T. B. Massalski, Phys. Rev. 138 Aa34 (1965).

FIGURE CAPTIONS

Part II

1. The heat capacities of copper-manganese alloys with 0.14 and 0.057 at.% Mn, respectively. The T^{-4} term of the dashed curve was calculated from the corresponding T^{-2} term determined in the straight-line region at higher temperatures.
2. The heat capacities of copper-manganese alloys with 3.19, 1.07, and 0.59 at.% Mn, respectively. The T^{-4} term of the dashed curve was calculated from the corresponding T^{-2} term determined in the straight-line region at higher temperatures.
3. The electronic and magnetic heat capacities of dilute manganese in copper alloys.
4. The heat capacities of γ-manganese and copper-manganese alloys with 93.9, 58.6, and 43.5 at.% Mn, respectively.
5. The hyperfine field H_e at Mn nuclei as a function of the manganese content for the copper-manganese system.

APPENDIX

Low Temperature Heat Capacities of Manganin, Constantan and a Tungsten-Platinum Alloy

Manganin and constantan -- which are commonly used in low-temperature calorimetry for heater wire, and for heat and thermometer leads -- have large heat capacities and it is necessary to know these values so that corrections can be made to calorimetric data. It is particularly important below 1°K where these materials have hyperfine heat capacity contributions which become large compared with the usual lattice and electronic contributions. For the same reason they are not suitable for measurements below about 0.1°K on samples that have small heat capacities; the correction for the heat capacity of the heater and that part of the leads included in the measured heat capacity, in extreme cases, can limit the attainable accuracy. It has been found that a 9%W-91%Pt alloy, with a smaller heat capacity, is a substantial improvement over manganin and constantan in this respect. Giauque et al.[1] have already used this alloy for heater wire between 1 and 4°K, and have shown that it has conveniently low temperature and magnetic-field coefficients of electrical resistance. We have extended the resistivity measurements to 0.05°K and have found that the small negative temperature coefficient reported by Giauque et al. persists to this temperature. (It is possible that a superconducting transition might be found at a lower temperature.[2]) The alloy also has a very low thermal conductivity.[3]

Both manganin and constantan samples were obtained from the Driver-Harris Company and the tungsten-platinum alloy sample from Engelhard Industries. Each sample was cylindrical in shape and was fabricated from

the material used in the manufacture of the resistance wire. The stated compositions were 13% Mn-4% Ni-83% Cu, 43% Ni-57% Cu, and 9% W-91% Pt for manganin, constantan, and the tungsten-platinum alloy, respectively.

Smooth curves giving heat capacity versus temperature are shown in Fig. 1. With the exception noted below, the experimental points fell within 1% of the curves for manganin and constantan, and 2% at the lowest temperatures and 1% above 0.2°K for the tungsten-platinum alloy. For manganin the data between 0.2 (the lowest temperature of measurement) and 2.5°K are given by

$$C(\text{mJ g}^{-1}\text{ deg}^{-1}) = 0.00294T^{3} + 0.0595T + 0.0115T^{-2}. \qquad (1)$$

At temperatures above 2.5°K the data deviate from this equation, and smoothed values are given in Table 1. For constantan irreproducible heat capacities and spontaneous generation of heat in the sample were observed for temperatures between 0.3 and 1°K. These effects may have been associated with the exposure of the sample to a magnetic field of several thousand oersteds on cooling. From 0.15 (the lowest temperature of measurement) to 0.3°K the data are given by

$$C(\text{mJ g}^{-1}\text{ deg}^{-1}) = 0.205T + 0.00281T^{-2}. \qquad (2)$$

Smoothed values of the heat capacity at higher temperatures are given in Table 2. The experimental points in the region of 0.3 to 1.0°K deviated from the smoothed values by as much as 20%. For the tungsten-platinum alloy the data between 0.07 and 1.2°K, the whole temperature range at which measurements were made, can be represented by

$$C(\text{mJ g}^{-1}\text{ deg}^{-1}) = 0.0014T^{3} + 0.176T + 0.000012T^{-2}. \qquad (3)$$

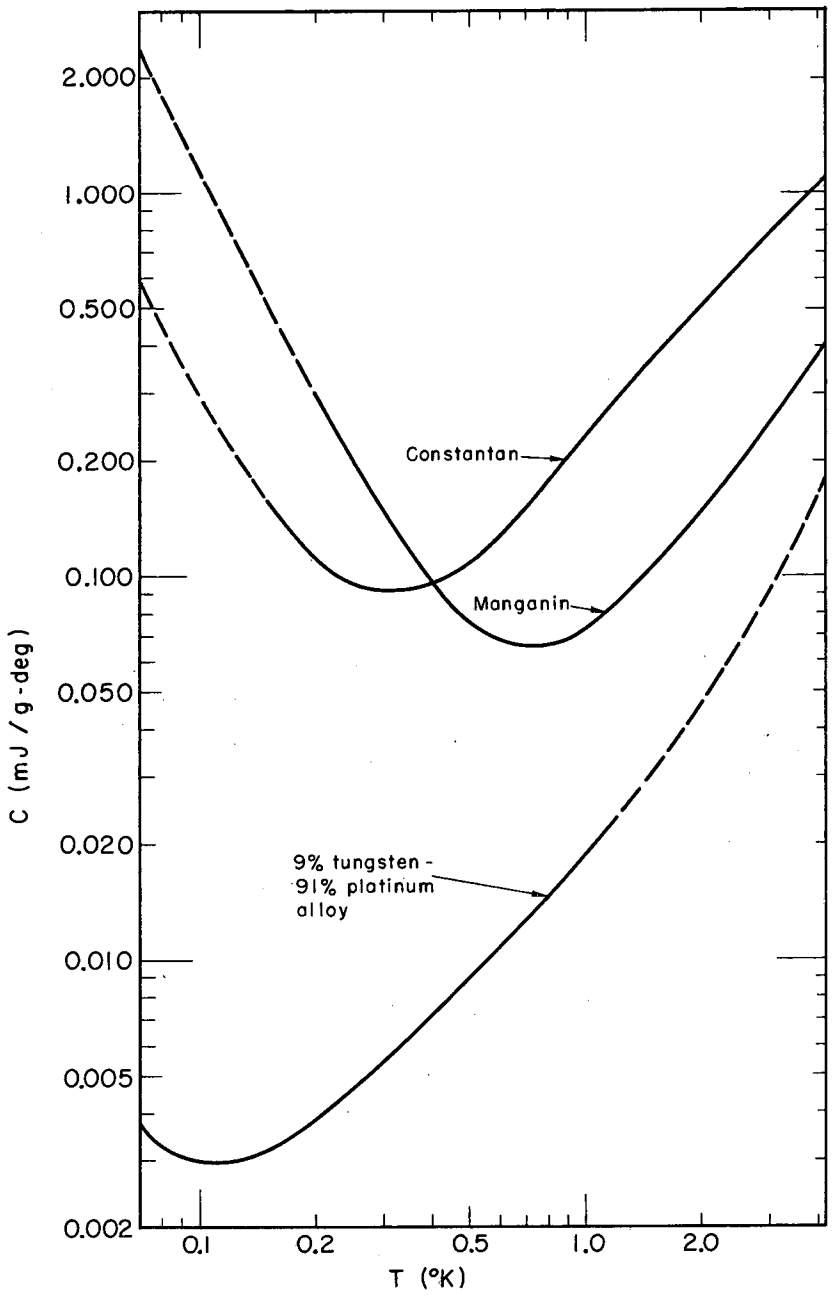
2.000
1.000
0.500
0.200
0.100
0.050
0.020
0.010
0.005
0.002
C (mJ / g-deg)
0.1
0.2
0.5
1.0
2.0
T (°K)
Constantan
Manganin
9% tungsten -
91% platinum
alloy
MUB-6288

Fig. 1

Table 1 Heat capacity of manganin

T (°K)	C (millijoules/gram-degree)
< 2.50	$0.0115T^{-2} + 0.0595T + 0.0294T^{3}$
2.50	0.197
2.75	0.224
3.00	0.251
3.25	0.280
3.50	0.310
3.75	0.342
4.00	0.376

Table 2 Heat capacity of constantan

T (°K)	C (millijoules/gram-degree)
< 0.30	$0.00281T^{-2} + 0.205T$
0.30	0.0927
0.40	0.0960
0.50	0.107
0.75	0.163
1.00	0.233
1.25	0.303
1.50	0.372
1.75	0.442
2.00	0.511
2.25	0.580
2.50	0.649
2.75	0.715
3.00	0.786
3.25	0.853
3.50	0.923
3.75	0.991
4.00	1.060

For manganin the hyperfine heat capacity seems reasonable compared with those values for the copper-manganese systems alloys described in Part II. For constantan the observed T^{-2} term corresponds to an H_e of 100 kOe at Cu nuclei. (Since only about 1% of the Ni nuclei have non-zero spin and they have very small magnetic moment, the contribution from Ni nuclei, even with an H_e of the same magnitude as that in the pure nickel metal, will be still less than one tenth of one percent of the observed T^{-2} term.) However, according to the NMR work for copper-nickel alloys by Asayama et al.[4] and Asayama,[5] the hyperfine fields at both Cu and Ni nuclei should become very small in the alloy with composition like constantan because the ferromagnetism disappears at about 40% Ni. This suggests that the observed T^{-2} term is much larger than that expected from the magnetic hyperfine origin and possibly arises from other mechanisms which might be connected to the irreproducible heat capacities and spontaneous generation of heat in the sample observed during the heat capacity measurements as mentioned above. For the tungsten-platinum alloy, we know of no reason to expect even the small observed T^{-2} term, and it seems likely that it, and possibly the resistance minimum is associated with the presence of a magnetic impurity. (Our samples and those of Giauque et al.[1] were all obtained from the same supplier.)

We have found 0.0009 in diameter tungsten-platinum wire a convenient size for electrical heaters and leads. This size is strong enough to present no great problems in handling, and it has a high electrical resistant (460 Ω/ft at 1°K). The bare wire was obtained from the Engelhard Industries[6] and Formvar insulation was applied by the Rea Magnet Company, Inc.[7]

REFERENCES

1. W. F. Giauque, D. N. Lyon, E. W. Hornung, and T. E. Hopkins, J. Chem. Phys. 37, 1446 (1962).

2. T. H. Geballe, B. T. Matthias, V. B. Compton, E. Corenzwit, and G. W. Hull, Jr., Phys. Rev. 129, 182 (1963).

3. A. J. Buhl and W. F. Giauque, Rev. Sci. Instr. 36, 703 (1965).

4. K. Asayama, S. Kobayashi, and J. Itoh, J. Phys. Soc. Japan 18, 458 (1963).

5. K. Asayama, J. Phys. Soc. Japan 18, 1727 (1963).

6. Baker Platinum Division, Engelhard Industries, Newark, New Jersey.

7. Rea Magnet Wire Company, Incorporated, Fort Wayne, Indiana.

FIGURE CAPTIONS

Appendix

1. The heat capacities of constantan, manganin and a 9%W-91%Pt alloy. The solid curves represent measured values, and the dashed curves, extrapolations.

ACKNOWLEDGMENTS

The author wises to express his sincere thanks to Professor Norman E. Phillips for his continuous guidance and encouragement through the work. He is also indebted to the following persons for kindly providing various samples: Dr. E. G. King and Dr. F. E. Block, Bureau of Mines, U. S. Department of the Interior (chromium); Mr. W. Bindloss, Department of Physics, University of California, Berkeley (gold-manganese); Dr. J. A. Cameron, Clarendon Laboratory, University of Oxford (osmium-iron); and Dr. J. E. Zimmerman, Scientific Laboratory, Ford-Motor Company (copper manganese).

The author is grateful to Dr. N. Benczer-Koller, Dr. J. R. Harris, and Dr. G. M. Rothberg, Department of Physics, Rutgers University, for generously making available to him their experimental results prior to publication.

This work was performed under the auspices of the United States Atomic Energy Commission.